Quantum kinetics of a superconducting tunnel junction: Theory and comparison with experiment

Kenneth S. Chow, Dana A. Browne, and Vinay Ambegaokar
Laboratory for Atomic and Solid State Physics, Clark Hall, Cornell University, Ithaca, New York 14853
(Received 17 July 1987)

We develop a kinetic theory for the real-time response of a quantum particle interacting with a macroscopic reservoir. We discuss the equilibrium and long-time behavior of the solution of the kinetic equation for such a system. In the limit of low damping, the kinetic equation reduces to a master equation. Using the theory to model a Josephson junction loaded with an external impedance, we make contact with the experiments of Clark, Devoret, Esteve, and Martinis. We argue that a stationary solution of the master equation sufficiently describes the experiments, and make detailed comparison with data.

I. INTRODUCTION

The quantum dynamics of the phase variable associated with weakly coupled superconductors is interesting both in its own right and because of its observable consequences.[1] On the one hand it is fascinating that a degree of freedom as abstract as the relative phase of the order parameters in two nearby superconductors can be shown,[2,3] using the standard theory of condensed matter, to obey quantum mechanics—albeit in the somewhat intricate form appropriate to a variable that is coupled to a dissipative environment; on the other, it is an important challenge to verify that this theoretical picture does, in fact, account for the results of increasingly delicate experiments.

Among the experiments one would like to explain in detail are some very beautiful ones[4–6] on the transition from the resistanceless to the resistive state in Josephson junctions driven by currents with and without microwave frequency modulation. A considerable effort was made in these measurements to determine parameters such as the resistance and capacitance *in situ*, with a view to minimizing the possibility of uncontrolled fits of theory to experiment. The aim of this paper is to examine these experiments in their general theoretical context.

In a recent article,[7] the present authors derived a fully quantum-mechanical kinetic equation governing the time development of the phase variable alluded to above, making only the assumption that the environment remains in equilibrium. We also took preliminary steps towards making contact with the experiments referred to above. It was shown that in the low-damping limit corresponding to the experiments and at low temperatures, when only the two lowest levels in the metastable quantum well describing the system (see Sec. III) are appreciably occupied, a numerical estimate without adjustable parameters, i.e., using values determined by the experimenters, gave, in a situation where the approximations were valid, good agreement with the measured width of a resonance corresponding to microwave-induced escape.

The present paper is a sequel to the above-mentioned article, and contains calculational details and many comparisons with experimental data. There are similarities between this work and a recent article by Larkin and Ovchinnikov.[8] Their starting point is a master equation, identical to the low-damping limit of our kinetic equation, which they had previously used[9] mainly to discuss the high-temperature limit. In Ref. 8, calculations based on this equation are done of the complete line shape for the resistanceless to resistive transition. Our present work has been heavily influenced by Ref. 8, but it goes beyond it as well. For those who have already mastered the work of Larkin and Ovchinnikov, it may be worth listing our new results.

(1) We have done calculations to compare theory and experiment for several sets of published experimental data that had not previously been so compared.

(2) Our calculations give insight into the inner workings of the theory, in particular to the question of how far the phase departs from equilibrium within the metastable well.

(3) By computerizing the calculation we have been able to model experiments planned but not yet done,[10] involving a modification of the dissipative environment, and to predict what should be observed.

The plan of this paper is as follows. In the next section we derive the kinetic equation. We start from the Caldeira-Leggett model.[1] We discuss both equilibrium and time dependence. Like all quantum transport equations, ours is not useful until some approximation is introduced for the collision processes. We specialize to the "self-consistent Born approximation," appropriate to the low-damping limit and show how a well-known effect, the environment-induced shrinking of the size of the quantum state in a harmonic well, emerges. We then show how in the approximation of slow time dependence the kinetic equation reduces to a master equation, including energy shifts due to interaction with the environment. In Sec. III the master equation is applied to the problem of escape from a metastable well, corresponding to the resistanceless to resistive transition discussed

above. We assume that the most important effect of dissipation consists in level shifts and in transitions between levels within the well, and we therefore ignore the environment in calculating the escape from the well. Our calculation of level positions, widths, and matrix elements is influenced by Ref. 8 but is different in detail. We then use these elements to calculate a time-independent current-carrying solution of the master equation corresponding to a steady leakage of probability from inside the well, both in the presence and in the absence of applied microwaves. In Sec. IV we consider dissipative environments more general than Ohmic resistances. In particular, we calculate the effect of placing a transmission line across the junction, in a manner planned by the experimentalists.[10] Section V contains results of our calculation with comparison to experimental data.[5,11] There are two appendices. In Appendix A we give a pedagogic discussion of the equilibrium solution of the kinetic equation. Appendix B contains some calculational details.

II. KINETIC THEORY

In this section we will present an approach[7] to the real-time dynamics of a quantum particle interacting with a dissipative environment in terms of a kinetic equation for a quantity that is closely related to the reduced density matrix for the particle. Our equation is formally identical to that found in theories of many-body quantum transport, but differs in certain details. It is not possible in general to write a kinetic equation for the density matrix alone because at low temperatures the bath does not lose memory of the past history of the particle motion rapidly enough.

There has recently been other work[12,13] devoted to developing equations for the real-time response that are based on the Keldysh formulation of transport theory.[14] In that work, the potential felt by the particle is broken into a piece for which the path integral including the bath can be explicitly evaluated, and a remainder whose effect is accounted for in perturbation theory. We will take the complementary approach of assuming that the problem of the quantum motion of the isolated particle has been solved, and study the effect of dissipation on the particle motion via an expansion in the strength of the particle-bath coupling. Thus our theory[7] is ideally suited to discuss the weak-damping limit for a general one-body potential.

We assume that the combined system of particle and bath is governed by the Hamiltonian

$$H = H_0 + \sum_i \omega_i \alpha_i^\dagger a_i - \sum_i C_i x_i q + \sum_i \frac{C_i^2}{2m_i\omega_i} q^2 , \tag{2.1}$$

where H_0 is the Hamiltonian of the isolated particle, the second term describes the reservoir as a collection of harmonic oscillators, and the last two describe the coupling between the particle and the bath. Here C_i is the strength of the coupling, $x_i = [1/(2m_i\omega_i)]^{1/2}(a_i^\dagger + a_i)$ and q are the bath and particle coordinates, respectively, and the last term is a counter term to remove a bath-induced change in the static potential seen by the particle.[1,15] Such an effective Hamiltonian has been justified for the Josephson junction with the damping due to quasiparticle tunneling by Ambegaokar *et al.*[3,16]

The density matrix ρ of the combined system is given in the interaction representation by

$$\rho(t) = U(t,0)\rho(0)U^\dagger(t,0) . \tag{2.2}$$

The time evolution operator $U(t,t')$ is given by

$$U(t,t') = \exp(-iH_0 t) T_t \left[\exp\left[-i \int_{t'}^{t} V_I(\tau) d\tau \right] \right] \times \exp(iH_0 t') , \tag{2.3}$$

where T_t denotes the time-ordering operator and $V_I(t)$ is the sum of the two particle-bath coupling terms in the interaction representation.

Since we are interested solely in the properties of the particle, we define the reduced density matrix $\hat{\rho}$ by $\hat{\rho}(t) = \mathrm{Tr}[\rho(t)]$ where the Tr denotes a trace over the bath variables. In general, it is not possible to write a kinetic equation for $\hat{\rho}$ in terms of itself because the bath does not respond instantaneously to the motion of the particles. We therefore define a two-time Green function by

$$\hat{G}(t_1,t_2) = \mathrm{Tr}[U(t_1,0)\rho(0)U^\dagger(t_2,0)] \tag{2.4}$$

which for $t_1 = t_2$ is the density matrix. We also introduced the retarded and advanced Green functions

$$\begin{aligned} G^r(t_1,t_2) &= -i\Theta(t_1-t_2)\mathrm{Tr}[U(t_1,t_2)\rho_{\mathrm{eq}}^{\mathrm{bath}}] , \\ G^a(t_1,t_2) &= +i\Theta(t_2-t_1)\mathrm{Tr}[U(t_1,t_2)\rho_{\mathrm{eq}}^{\mathrm{bath}}] , \end{aligned} \tag{2.5}$$

which describe the modification of the time evolution of the quantum particle due to its coupling to the bath. The propagators for the decoupled particle are denoted $G_0^{r,a}$.

We now expand U in Eqs. (2.4) and (2.5) in powers of V_I and perform the trace over the bath. The nth term in the expansion requires the evaluation of a correlation function of n bath coordinates $x_i(t)$. Since we assume the initial density matrix $\rho(0)$ describes the bath as being in thermal equilibrium in the distant past, this correlation function can be reduced to a sum over all distinct products of the two-time pair correlation functions of the bath variables given by

$$\begin{aligned} \alpha(t,t') &= \sum_i C_i^2 \langle x_i(t) x_i(t') \rangle , \\ &= \int_{-\infty}^{\infty} \frac{d\omega}{\pi} J(\omega)[1+n(\omega)] e^{-i\omega(t-t')} , \end{aligned} \tag{2.6}$$

where $n(\omega) = 1/[\exp(\beta\omega)-1]$ is the Bose distribution function and we have defined the bath spectral function

$$J(\omega) = \pi \sum_i \frac{C_i^2}{2m_i\omega_i} \delta(\omega-\omega_i) . \tag{2.7}$$

If we were to assume that in the classical limit the particle experiences a friction force linear in the velocity, we would find that[1] $J(\omega) = m\gamma\omega\Theta(\omega_c - |\omega|)$, where $m\gamma$ is the classical coefficient of friction, m is the mass of the particle, and ω_c is a high-frequency cutoff.

In the usual way, $\hat{G}$, G^r, and G^a obey Dyson equations, which define the self-energy operators $\hat{\sigma}$, σ^r, and σ^a

$$G^{r,a}(t_1,t_2)=G_0^{r,a}(t_1,t_2)+\int_{-\infty}^{\infty}dt_1'\int_{-\infty}^{\infty}dt_2' G_0^{r,a}(t_1,t_1')\sigma^{r,a}(t_1',t_2')G^{r,a}(t_2',t_2) \tag{2.8}$$

and

$$\hat{G}(t_1,t_2)=G^r(t_1,0)\hat{\rho}(0)G^a(0,t_2)+\int_{-\infty}^{\infty}dt_1'\int_{-\infty}^{\infty}dt_2' G^r(t_1,t_1')\hat{\sigma}(t_1',t_2')G^a(t_2',t_2)\ . \tag{2.9}$$

In addition to the integration over time, each product in the above equations also denotes an internal integration over the particle coordinate which we will do by summing over a complete set of states that diagonalize H_0. The quantities in Eq. (2.9) should therefore be regarded as matrices in the basis of particle states.

The above equations have the same structure as those used in the quantum kinetic theory of many-body transport,[14] the principal difference being that the self-energies $\sigma^{r,a}$ and $\hat{\sigma}$ in our formalism have no terms corresponding to "exchange" or "particle-hole annihilation" processes because we are treating one particle, not several, and there is no way to impose quantum statistics upon it. With this one difference, it is obvious that the Feynman diagrammatic approach can be applied here as well.

In order to express the above equations in the form of a kinetic equation, we differentiate Eq. (2.9) with respect to t_1 and t_2 and add to find a kinetic equation

$$i\left[\frac{\partial}{\partial t_1}+\frac{\partial}{\partial t_2}\right]\hat{G}(t_1,t_2)-[H_0+\mathrm{Re}\,\sigma,\hat{G}]-[\hat{\sigma},\mathrm{Re}\,g]=\frac{i}{2}\{A,\hat{\sigma}\}-\frac{i}{2}\{\Gamma,\hat{G}\}\ , \tag{2.10}$$

where the square brackets denote a commutator and the curly braces an anticommutator. We have defined $G^{r,a}=\mathrm{Re}\,g\mp iA/2$, and $\sigma^{r,a}=\mathrm{Re}\sigma\mp i\Gamma/2$. A is the spectral weight function which can be written

$$A(1,2)=\sum_n e^{-iE_n(t_1-t_2)}\Psi_n(x_1)\Psi_n^*(x_2) \tag{2.11}$$

for the uncoupled particle with eigenstates Ψ_n. The terms on the left-hand side of Eq. (2.10) with $\mathrm{Re}\,g$ and $\mathrm{Re}\,\sigma$ are corrections to the single-particle properties akin to the wave-function renormalization factor in many-particle systems. The anticommutator with Γ is the "scattering out" term that arises from the decay of amplitude from one state into others, while the term with $\hat{\sigma}$ represents "scattering in" to a given state from other states.

To cast the above equation into a simpler form, it is useful to introduce a distribution function $f(1,2)$ by

$$\hat{G}(1,2)=i[G^r(1,3)f(3,2)-f(1,3)G^a(3,2)]\ .$$

Then (2.10) can be rewritten as

$$i\left[\frac{\partial}{\partial t_1}+\frac{\partial}{\partial t_2}\right]f(t_1,t_2)-[H_0+\mathrm{Re}\sigma,f]=i\hat{\sigma}-\frac{i}{2}\{\Gamma,f\}\ . \tag{2.12}$$

Because of the rather unfamiliar form of these equations, we will examine the kinetic equation (2.10) and the Dyson equation (2.8) to leading order in the bath coupling. This results in the self-consistent Born approximation, where the self-energies $\sigma^{r,a}$ and $\hat{\sigma}$ are given by

$$\begin{aligned}\sigma^{r,a}(t_1,t_2)&=\alpha(t_1-t_2)q_{\mathrm{op}}G^{r,a}(t_1,t_2)q_{\mathrm{op}}\\&\quad+\delta(t_1-t_2)\int_0^{\infty}\frac{d\omega}{\pi\omega}J(\omega)(q_{\mathrm{op}})^2\ ,\\ \hat{\sigma}(t_1,t_2)&=\alpha(t_2-t_1)q_{\mathrm{op}}\hat{G}(t_1,t_2)q_{\mathrm{op}}\ ,\end{aligned} \tag{2.13}$$

where q_{op} is the position operator of the particle.

We will begin by discussing the information contained in the retarded function G^r. In the absence of a time-dependent external potential, it is clear that $G^r(t_1,t_2)$ is a function of t_1-t_2. Its Fourier transform is given by

$$G^r_{mn}(\omega)=\left[\omega-H_0-\mathrm{Re}\,\sigma+\frac{i}{2}\Gamma\right]^{-1}_{mn}\ , \tag{2.14}$$

where the subscripts denote the matrix element in a set of basis functions that, for example, diagonalize H_0. The spectral function $A_{mn}(\omega)=-2\,\mathrm{Im}G^r_{mn}(\omega)$ will, if the coupling to the bath is small enough, have sharp peaks as a function of ω which represent "quasi-eigenstates" for the particle in the presence of the bath. These quanti-stationary states have a width that arises because the coupling to the bath will eventually cause the particle amplitude to leak away into other states. The energy of these states will also be shifted by the bath, akin to the Lamb shift in the hydrogen caused by the vacuum fluctuations in the electromagnetic field. If the coupling is small enough, we can find the position of these poles in G^r by keeping only the diagonal components of the self-energy. Thus the new energy Ω_n is given by

$$\Omega_n=E_n+\mathrm{Re}\,\sigma_{nn}(\Omega_n) \tag{2.15}$$

and the decay width by

$$\gamma_n\simeq\left.\frac{\Gamma_{nn}}{1-\dfrac{\partial\mathrm{Re}\,\sigma_{nn}(\omega)}{\partial\omega}}\right|_{\omega=\Omega_n}\ . \tag{2.16}$$

As an example, we will calculate the level shift and width of an harmonic oscillator coupled to a heat bath. In lowest order, the energy shift is

$$\mathrm{Re}\,\sigma_{nn}(E_n)=\sum_k |\langle n|q|k\rangle|^2 \times\int_{-\infty}^{\infty}\frac{d\omega}{\pi}J(\omega)\times\left[\frac{1+n(\omega)}{E_n-\omega-E_k}+\frac{\Theta(\omega)}{\omega}\right] \tag{2.17}$$

and the lifetime is

$$\Gamma_{nn}(E_n)=2\sum_k \langle n|q|k\rangle|^2 J(E_n-E_k)\times[1+n(E_n-E_k)]\,. \tag{2.18}$$

Using the harmonic oscillator matrix elements we find a complex energy shift for the kth level

$$\delta E_k+i\frac{\Gamma_k}{2}=\int_0^{\infty}\frac{d\omega}{2\pi m}\mathrm{Re}\,Y(\omega)\left[\frac{1+k}{\omega+\Omega}+\omega n(\omega)\frac{2}{\omega^2-\Omega^2}\right]+i\frac{\mathrm{Re}\,Y(\Omega)}{2m}n(\Omega) +\frac{k}{2m}\left[\mathrm{Im}\,Y(\Omega)+i\mathrm{Re}\,Y(\Omega)\coth\left[\frac{\Omega}{2k_BT}\right]\right], \tag{2.19}$$

where we have defined

$$\mathrm{Re}\,Y(\omega)=\frac{J(\omega)}{\omega}\,,\qquad \mathrm{Im}\,Y(\omega)=\int\frac{d\omega'}{\pi}\frac{\mathrm{Re}\,Y(\omega')}{\omega-\omega'}\,. \tag{2.20}$$

Note that if $\mathrm{Re}\,Y(\omega)=$const, as with Ohmic dissipation, then Im Y vanishes and we have only a constant shift of all the levels but they remain with their uncoupled separation, in agreement with Refs. 11 and 17. This lack of a Lamb shift is due to the fact that $J(\omega)$ is linear in ω (Ohmic dissipation) and that the uncoupled eigenstates are evenly spaced in energy. In any model where the above two conditions are not met, as for example in a superconducting quantum interference device (SQUID) with dissipation caused by quasiparticle tunneling or for a Josephson junction coupled to a transmission line, there will be a dissipation-induced Lamb shift. Note also that the change in frequency is independent of temperature, while the lifetime is temperature dependent.

Before discussing the nonequilibrium response, we will examine the information contained in the equilibrium Green function $\hat{G}$. In equilibrium, we expect that $\hat{G}$ and G^r are functions only of the difference in their time arguments. If we Fourier transform the Green functions with respect to this time difference, Eq. (2.10) becomes

$$-[H_0+\mathrm{Re}\,\sigma(\omega),\hat{G}(\omega)]-[\hat{\sigma}(\omega),\mathrm{Re}\,g(\omega)] =\frac{i}{2}\{A(\omega),\hat{\sigma}(\omega)\}-\frac{i}{2}\{\Gamma(\omega),\hat{G}(\omega)\}\,. \tag{2.21}$$

Since all quantities in the above equation are real, both sides must vanish in equilibrium. Let us make the ansatz $\hat{G}_{mn}(\omega)=f_e(\omega)A_{mn}(\omega)$, where $f_e(\omega)$ is the equilibrium distribution function. From the Dyson equation (2.8) and its conjugate, we see that in equilibrium

$$[H_0+\mathrm{Re}\sigma(\omega),A(\omega)]=-[\Gamma(\omega),\mathrm{Re}g(\omega)]\,. \tag{2.22}$$

Using this result, we find that if (2.21) is to vanish, $\hat{\sigma}_{mn}(\omega)=f_e(\omega)\Gamma_{mn}(\omega)$. One suspects that $f_e(\omega)\propto\exp(-\beta\omega)$, which we will show for the self-consistent Born approximation. The result is actually true to all orders in the coupling (see Appendix A). Fourier transforming the above, we find

$$\sigma^{r,a}(\omega)=\int_{-\infty}^{\infty}\frac{d\omega'}{\pi}J(\omega')[1+n(\omega')]q_{\mathrm{op}}G^{r,a}(\omega-\omega')q_{\mathrm{op}} +\int_0^{\infty}\frac{d\omega}{\pi\omega}J(\omega)(q_{\mathrm{op}})^2\,, \qquad \hat{\sigma}(\omega)=\int_{-\infty}^{\infty}\frac{d\omega'}{\pi}J(\omega')n(\omega')q_{\mathrm{op}}\hat{G}(\omega-\omega')q_{\mathrm{op}}\,. \tag{2.23}$$

Using our forms for $\hat{G}$ and $\hat{\sigma}$ we find that the solution is indeed $f_e(\omega)=\mathrm{const}\exp(-\beta\omega)$. The constant can be determined from the condition

$$\mathrm{tr}\hat{\rho}=\mathrm{const}\times\int(d\omega/2\pi)\exp(-\beta\omega)\mathrm{tr}\,A(\omega)=1\,. \tag{2.24}$$

where tr denotes tracing over the particle coordinate. Thus we find in equilibrium that $\hat{G}$ and $\hat{\sigma}$ are given by

$$\hat{G}(\omega)=\exp[-(\beta\omega)]A(\omega)/Z\,,\qquad \hat{\sigma}(\omega)=\exp[-(\beta\omega)]\Gamma(\omega)/Z\,, \tag{2.25}$$

where $Z=\int(d\omega/2\pi)\exp(-\beta\omega)\mathrm{tr}\,A(\omega)$ is the partition function of the particle.

We now consider the dissipation-induced changes in the equilibrium density matrix. In order to develop closed form expressions we will on occasion ignore the self-consistency requirements. To calculate the change in the density matrix, we will need expressions for the change in the spectral weight $A_{mn}(\omega)$. We start from the expression

$$A_{mn}(\omega)=-2\mathrm{Im}\left[\omega-H_0-\mathrm{Re}\,\sigma(\omega)+\frac{i}{2}\Gamma(\omega)\right]^{-1}_{mn}\,. \tag{2.26}$$

The change in A to leading order is given by

$$\delta A_{mn}(\omega)=-2\mathrm{Im}\delta G^r_{mn}(\omega)\,, =-2\mathrm{Im}\frac{1}{\omega-E_m+i\delta}\sigma^r{}_{mn}(\omega)G^r_{nn}(\omega)\,. \tag{2.27}$$

For $m\neq n$ we can replace G^r with G^r_0 to obtain

$$\delta A_{mn}(\omega)=\frac{2\pi[\delta(\omega-E_n)-\delta(\omega-E_m)]\mathrm{Re}\,\sigma_{mn}(\omega)}{E_n-E_m}+\frac{\Gamma_{mn}(\omega)}{(\omega-E_n)(\omega-E_m)}\ . \tag{2.28}$$

For $m=n$ the singular behavior for $\omega=E_n$ must be treated carefully. The result can be obtained by formally taking the limit $E_n\to E_m$ in the above equation which gives

$$\delta A_{nn}(\omega)=2\pi\delta(\omega-E_n)\frac{\partial\mathrm{Re}\,\sigma_{nn}(\omega)}{\partial\omega}+\frac{\Gamma_{nn}(\omega)}{(\omega-E_n)^2}\ . \tag{2.29}$$

The first term is the reduction of the spectral weight of the "quasieigenstate." Note that $\int d\omega\,\mathrm{tr}\,\delta A=0$ so the partition function is unchanged to this order.

We can now calculate the change in the density matrix $\delta\hat{\rho}=\int(d\omega/2\pi)\exp(-\beta\omega)\delta A(\omega)$. We find that the diagonal elements are given by

$$\delta\hat{\rho}_{nn}=e^{-\beta E_n}\frac{\partial\mathrm{Re}\sigma_{nn}(\omega)}{\partial\omega}\bigg|_{\omega=E_n}+\sum_k|\langle n\,|\,q\,|\,k\rangle|^2e^{-\beta E_k}\times\int\frac{d\omega}{\pi}\frac{J(\omega)[1+n(\omega)]}{(\omega+E_n-E_k)^2} \tag{2.30}$$

and the off-diagonal elements are given by

$$\delta\hat{\rho}_{nm}=\frac{e^{-\beta E_n}\mathrm{Re}\sigma_{nm}(E_n)-e^{-\beta E_m}\mathrm{Re}\sigma_{nm}(E_m)}{E_n-E_m}+\sum_k\langle n\,|\,q\,|\,k\rangle\langle k\,|\,q\,|\,m\rangle e^{-\beta E_k}\times\int\frac{d\omega}{\pi}\frac{J(\omega)[1+n(\omega)]}{(\omega+E_n-E_k)(\omega+E_m-E_k)}\ . \tag{2.31}$$

Let us turn again to the simple model of the harmonic oscillator coupled to a thermal bath and compute the change in the width of the oscillator $\langle q^2\rangle$ due to the environment. For the simple harmonic oscillator we see immediately that only $\delta\hat{\rho}_{nn}$ and $\delta\hat{\rho}_{n,n\pm2}$ are nonzero to this order. Then we find

$$\delta\langle q^2\rangle=\frac{1}{2m\Omega}\{2I_0+[2+e^{-\beta\Omega}+n(\Omega)]\times[I_1-(1+e^{-\beta\Omega})I_2]\}\ , \tag{2.32}$$

where

$$I_0=\frac{1}{2m\Omega}\int_{-\infty}^{\infty}\frac{d\omega}{\pi}J(\omega)\frac{1+n(\omega)(1-e^{-\beta\Omega})}{(\omega+\Omega)^2}\ ,$$
$$I_1=\frac{1}{2m\Omega^2}\int_{-\infty}^{\infty}\frac{d\omega}{\pi}J(\omega)\frac{1+n(\omega)(1-e^{-\beta\Omega})}{\omega+\Omega}\ , \tag{2.33}$$
$$I_2=\frac{1}{2m\Omega^2}\int_0^{\infty}\frac{d\omega}{\pi}\frac{J(\omega)}{\omega}\ .$$

If we consider low temperatures and neglect terms of order $\exp(-\beta\Omega)$, we find

$$\delta\langle q^2\rangle=\frac{1}{2m\Omega}\int_0^{\infty}\frac{d\omega}{\pi}\frac{J(\omega)}{m}\left[-\frac{1}{\omega(\omega+\Omega)^2}+\frac{4\Omega n(\omega)}{(\Omega^2-\omega^2)^2}\right], \tag{2.34}$$

which for Ohmic dissipation $[J(\omega)=m\gamma\omega]$ reduces to

$$\delta\langle q^2\rangle=-\frac{1}{2m\Omega}\frac{\gamma}{\pi\Omega}\left[1-4\zeta(2)\left[\frac{T}{\Omega}\right]^2\right]. \tag{2.35}$$

Thus at $T=0$ the uncertainty in the particle's coordinate is reduced by the constant "measurement" of the coordinate by the bath. As the temperature increases, this contraction effect falls as the square of the temperature as the particle samples higher excited states. This is the source of T^2 enhancement of the tunneling rate out of the quadratic plus cubic potential. The above result agrees with the result derived with path integral techniques by Caldeira and Leggett.[1]

We now turn to understanding the nonequilibrium behavior contained in the kinetic equation. There is a great deal of information buried in the compact notation, but we are primarily interested in the low-frequency dynamics contained in the kinetic equation (2.10). By this we mean that we are interested in behavior that occurs on a time scale much longer than the inverse of the typical energy splitting in the quantum system. Also we would prefer to have an equation for the density matrix alone rather than this more complicated equation for $\hat{G}$. Our prejudice is that on long-time scales we can think of the motion of the system as being determined by a local density matrix that is uncorrelated with its value at times in the distant past. To be more precise, let us define an average time $T=(t_1+t_2)/2$ and a relative time $\tau=(t_1-t_2)$. Since, in equilibrium, all quantities are independent of T, we mean by "slowly varying" that the evolution as a function of T is slow on a scale set by the splitting of the energy levels. We will then find an equation for $\hat{\rho}(T)$ by performing a gradient expansion with respect to T in the kinetic equation.

The equation in its present form has a great deal of rapid variation in the off-diagonal components solely due to the term $[H_0,\hat{G}]$, since the off-diagonal components of the density matrix (which are nonzero due to the bath coupling as we showed above) then vary as $\exp[i(E_m-E_n)T]$. We therefore will transform to an "interaction picture" by the following transformation: If $Y(t_1,t_2)$ is some function, its interaction picture version is given by

$$Y(t_1,t_2)=e^{-iH_0t_1}Y_I(t_1,t_2)e^{iH_0t_2}\ . \tag{2.36}$$

We will also write the same quantity in the interaction representation in terms of T and τ as

$$Y_I\left[T+\frac{\tau}{2},T-\frac{\tau}{2}\right]=\int_{-\infty}^{\infty}d\omega\,Y_I[T;\omega]e^{-i\omega\tau}\ . \tag{2.37}$$

We will drop the subscript I in what follows.

In the interaction picture, the kinetic equation (2.10) becomes

$$i\left(\frac{\partial}{\partial t_1}+\frac{\partial}{\partial t_2}\right)\hat{G}(t_1,t_2)=\int dt[\sigma^r(t_1,t)\hat{G}(t,t_2)+\hat{\sigma}(t_1,t)G^a(t,t_2)-\hat{G}(t_1,t)\sigma^a(t,t_2)-G^r(t_1,t)\hat{\sigma}(t,t_2)]\ . \tag{2.38}$$

In this representation, the Green functions for the noninteracting particle are given by

$$\begin{aligned} G^r[T;\omega]&=\frac{1}{2\pi}\frac{\sum_n |\,n\,\rangle\langle\,n\,|}{\omega+i\delta}\ , \\ \hat{G}[T;\omega]&=\delta(\omega)\sum_n \exp(-\beta E_n)\,|\,n\,\rangle\langle\,n\,|\ . \end{aligned} \tag{2.39}$$

Consider now the self-energies. In our Born approximation and including an external potential $V(t)$ we have

$$\begin{aligned} \sigma^r_{nm}(t_1,t_2)&=\alpha(t_1-t_2)\langle n\,|\,q_{\rm op}\,|\,k\,\rangle G^r_{kl}(t_1,t_2)\langle l\,|\,q_{\rm op}\,|\,m\,\rangle e^{i(E_n-E_k)t_1+i(E_l-E_m)t_2} \\ &\quad+\delta(t_1-t_2)\int_0^\infty\frac{d\omega}{\pi\omega}J(\omega)\langle n\,|\,(q_{\rm op})^2\,|\,m\,\rangle e^{i(E_n-E_m)t_1}+\langle n\,|\,V(t_1)\,|\,m\,\rangle\delta(t_1-t_2)e^{i(E_n-E_m)t_1}\ , \\ \hat{\sigma}_{nm}(t_1,t_2)&=\alpha(t_2-t_1)\langle n\,|\,q_{\rm op}\,|\,k\,\rangle\hat{G}_{kl}(t_1,t_2)\langle l\,|\,q_{\rm op}\,|\,m\,\rangle e^{i(E_n-E_k)t_1+i(E_l-E_m)t_2}\ . \end{aligned} \tag{2.40}$$

Since the Green functions are assumed to be smooth functions of $T=(t_1+t_2)/2$, the self-energies will be a slowly varying function of T only if the factor $(E_n-E_k+E_l-E_m)$ is small compared to the typical level spacing. Hence we will keep only those terms where the phase factor is small, which if there is no regularity in the level spacing requires that (1) ($n=m$ and $k=l$) or (2) ($n=k$ and $m=l$). This is usually called the "secular" approximation. Note that this implies that the only important bath contributions to the retarded self-energies are those diagonal in the basis if the bath coupling is weak. The perturbation $V(t)\propto\cos(\omega t)$ is only slowly varying if $E_n-E_m\pm\omega\simeq 0$. These terms are obviously nearly in resonance. Keeping only those terms is tantamount to the "rotating wave" approximation. In the absence of an explicitly time-dependent potential, the retarded and advanced functions are automatically independent of the "center-of-mass" time T.

We can therefore expand (2.38) in gradients of T. Keeping only the lowest-order terms gives

$$\frac{\partial}{\partial T}\hat{G}_{mn}[T;\omega]=-2\pi i\sum_k\{\sigma^r_{mk}[T;\omega]\hat{G}_{kn}[T;\omega]-\hat{G}_{mk}[T;\omega]\sigma^a_{kn}[T;\omega]+\hat{\sigma}_{mk}[T;\omega]G^a_{kn}[T;\omega]-G^r_{mk}[T;\omega]\hat{\sigma}_{kn}[T;\omega]\}\cdot \tag{2.41}$$

The self-energies are given by

$$\begin{aligned} \sigma^r_{nm}[T;\omega]&=\int\frac{d\omega'}{\pi}J(\omega')[1+n(\omega')]\langle n\,|\,q_{\rm op}\,|\,k\,\rangle G^r_{kl}[T;\omega-\omega'+E_n-E_k]\langle l\,|\,q_{\rm op}\,|\,m\,\rangle \\ &\quad+\int_0^\infty\frac{d\omega'}{\pi\omega'}J(\omega')\langle n\,|\,(q_{\rm op})^2\,|\,m\,\rangle e^{i(E_n-E_m)T}+\langle n\,|\,V(T)\,|\,m\,\rangle e^{i(E_n-E_m)T}\ , \\ \hat{\sigma}_{nm}[T;\omega]&=\int\frac{d\omega'}{\pi}J(\omega')n(\omega')\langle n\,|\,q_{\rm op}\,|\,k\,\rangle\hat{G}_{kl}[T;\omega-\omega'+E_n-E_k]\langle l\,|\,q_{\rm op}\,|\,m\,\rangle\ . \end{aligned} \tag{2.42}$$

Let us now integrate over ω to find the equation of motion of the density matrix, since the unperturbed $\hat{G}$ is a sharp function of ω. If the coupling to the bath is weak, we expect $\hat{G}$ to sharply peaked function of ω on a scale of about the typical lifetime Γ found in (2.18). We expect that the spectral density $J(\omega)$ is slowly varying on the scale of Γ, so any quantity in (2.41) or (2.42) that multiplies $\hat{G}[T;\omega]$ can be evaluated at $\omega=0$. Thus we find

$$\frac{\partial}{\partial T}\hat{\rho}_{mn}[T]=-2\pi i\sum_k\{\sigma^r_{mk}[T]\hat{\rho}_{kn}[T]-\hat{\rho}_{mk}[T]\sigma^a_{kn}[T]+i\hat{\sigma}_{mn}[T]\}\ . \tag{2.43}$$

Finally, if we assume that the coupling is weak, we can replace the self-consistent retarded and/or advanced functions by the lowest-order terms

$$\begin{aligned} \sigma^r_{nm}[T]&=\int\frac{d\omega'}{\pi}J(\omega')[1+n(\omega')]\langle n\,|\,q_{\rm op}\,|\,k\,\rangle\frac{(2\pi)^{-1}}{E_n-\omega'-E_k+i0^+}\langle k\,|\,q_{\rm op}\,|\,m\,\rangle \\ &\quad+\int_0^\infty\frac{d\omega'}{\pi\omega'}J(\omega')\langle n\,|\,(q_{\rm op})^2\,|\,m\,\rangle e^{i(E_n-E_m)T}+\langle n\,|\,V(T)\,|\,m\,\rangle e^{i(E_n-E_m)T}\ , \end{aligned} \tag{2.44}$$

and using the peaked nature of $\hat{G}$ we find

$$\hat{\sigma}_{nm}[T]=\frac{1}{\pi}J(E_n-E_k)n(E_n-E_k)\times\langle n\mid q_{\rm op}\mid k\rangle\hat{\rho}_{kl}[T]\langle l\mid q_{\rm op}\mid m\rangle\ . \quad (2.45)$$

Equations (2.43)–(2.45) constitute a kinetic equation akin to the master equation. To see this, suppose that we ignore the self-consistency in the self-energies. Then the real part of σ_{nn} is given by

$$2\pi{\rm Re}\,\sigma_{nn}=\sum_k|\langle n\mid q_{\rm op}\mid k\rangle|^2\times\int_0^\infty\frac{d\omega}{\pi}J(\omega)\left[\frac{1+n(\omega)}{E_n-E_k-\omega}+\frac{n(\omega)}{E_n-E_k+\omega}+\frac{1}{\omega}\right] \quad (2.46)$$

which is nothing but the energy shift δE_n caused by the bath as calculated in second-order perturbation theory. Furthermore, let us define the usual golden-rule transition rates from state n to state m as

$$W_{n\to m}=2|\langle n\mid q_{\rm op}\mid m\rangle|^2J(E_n-E_m)[1+n(E_n-E_m)]\ . \quad (2.47)$$

These transition rates satisfy the detailed balance condition $W_{n\to m}/W_{m\to n}=\exp[-(E_m-E_n)/k_BT]$. We find from the kinetic equation (2.43) that the diagonal elements of the density matrix obey

$$\frac{d\hat{\rho}_{nn}(T)}{dT}=\sum_m W_{m\to n}\hat{\rho}_{mm}(T)-\left[\sum_m W_{n\to m}\right]\hat{\rho}_{nn}(T)-i\langle n\mid[V_I(T),\hat{\rho}(T)]\mid n\rangle\ , \quad (2.48)$$

where the scattering in and scattering out terms are clearly seen. The off-diagonal components of $\hat{\rho}$ evolve according to

$$\frac{d\hat{\rho}_{nm}(T)}{dT}=-\tfrac{1}{2}\sum_k(W_{m\to k}+W_{n\to k})\hat{\rho}_{nm}(T)-i(\delta E_n-\delta E_m)\hat{\rho}_{nm}(T)-i\langle n\mid[V_I(T),\hat{\rho}(T)]\mid m\rangle\ . \quad (2.49)$$

These equations are simply the master equation description of the quantum system. The net effect of the self-consistency is to alter the actual value of the relaxation rates and energy shifts, but the form of equations (2.48) and (2.49) is not changed significantly. In deriving these final equations we have assumed that the eigenvalues do not have any regularity in their spacing. For the harmonic oscillator, or for a nearly harmonic system, this is not true and we find additional terms for the off-diagonal elements which represent the transfer of coherence between one pair of levels and another pair. These terms turn out only to be more important in the classical limit where many levels are nearly in resonance. In that case, the full form of equation (2.46) for $\hat{\sigma}_{mn}$ must be used in the equation for the off-diagonal elements.

III. APPLICATION OF MASTER EQUATION

In this section we discuss how to make contact with experiments[4–6] by solving the master equation. For this reason, we have reinserted $\hbar$ everywhere it belongs. We begin with a brief description of the experimental setup and the correspondence between the experimental parameters and the parameters of the master equation. We then give a pedagogical account of the semiclassical method of calculating these parameters from the experimental inputs as outlined in Ref. 8. We supplement this with comparisons to numerical calculations of our own, to provide the reader with a feeling of the degree of accuracy of the semiclassical approximation in the present context and to point out its limits. Given all the parameters of the master equation, we then argue that a stationary solution adequately describes the experimental situation. We solve a simple model to illustrate the essential properties of this stationary solution before we present the general solution. In Sec. IV we discuss the various forms of dissipative mechanism of interest to us. Comparison to experimental data is deferred to Sec. V.

A typical experimental system[4–6] is a current-biased Josephson junction of capacitance C and critical current I_c. At bias current I_b the junction is described by the standard resistively shunted junction (RSJ) model as conducting via three channels: the supercurrent channel, the charge buildup in the capacitor, and the normal current through some general load with impedance $Z_{\rm load}$:

$$I_b=I_c\sin(\phi)+C\frac{dV}{dt}+\frac{V}{Z_{\rm load}}\ . \quad (3.1)$$

The voltage V is linked to the phase difference across the junction by the Josephson relation,

$$V=\frac{\hbar}{2e}\frac{d\phi}{dt}\ . \quad (3.2)$$

Equations (3.1) and (3.2) are equivalent to a "particle" with coordinate ϕ and mass $m=(\hbar/2e)^2C$ moving in a potential $V(\phi)=m\omega_J^2[1-\cos(\phi)]-(\hbar/2e)I_b\phi$, where $\omega_J^2=2eI_c/\hbar C$. Dissipation is introduced quantum mechanically by coupling the particle in the potential to a bath of oscillators as explained in Sec. II. When the current is close to being critical, the potential is well approximated by a metastable well of the form (see Fig. 1),

$$V(q)=3U\left[\frac{q}{q_0}\right]^2\left[1-\frac{2}{3}\frac{q}{q_0}\right]\ , \quad (3.3)$$

where

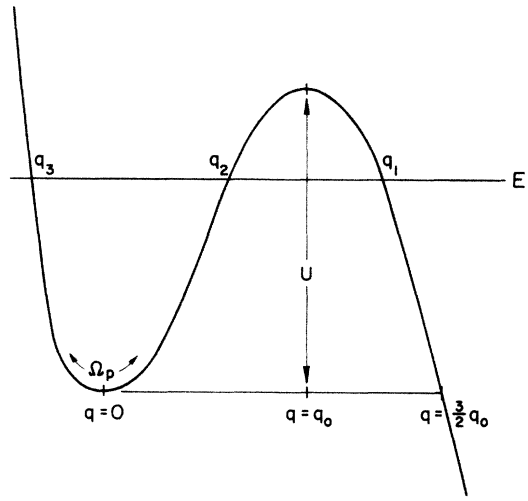

FIG. 1. Quadratic minus cubic potential as given in Eq. (3.3). q_1, q_2, and q_3 are the three turning points of classical motion at energy E.

$$q = \phi - \sin^{-1}(s) ,$$
$$s = I_b / I_c ,$$
$$U = m\Omega_p^2 q_0^2 / 6 ,$$
$$\Omega_p^2 = \omega_J^2 (1-s^2)^{1/2} ,$$
$$q_0^2 = 27 \left[1 - \frac{\cos^{-1}(s)}{(1-s^2)^{1/2}} \right] .$$

This defines the system of interest whose reduced density matrix we will be solving for. It is also of interest to examine the microwave enhancement of the particle escape rate from such a metastable potential.[5,6] In that case we add a term,

$$H_{\text{ext}} = -\frac{I_1 \hbar}{2e} \cos(\bar{\omega} t) q(t) \tag{3.4}$$

to the Hamiltonian, where $\bar{\omega}$ is the microwave frequency.

Given the shape of the potential and the damping spectral function $J(\omega)$, we need to compute three sets of quantities before we can go about solving the master equation (2.49). First, we need to define our basis set $\{n\}$ and to determine their energies relative to the well. We find it convenient to use a set of quasistationary states that are "inside the well" in some sense which will be explained later. The second set of quantities we need is, therefore, the widths of such states. The final parameters we need to compute are the bath-induced couplings $W_{k \to j}$ between the entries of the reduced density matrix.

In choosing a basis set for our solution, we will be considering the dissipationless particle in a potential. The effect of dissipation will be to modify the properties of such states without changing their fundamental nature. In particular, the shifts in energy and width of our basis states due to coupling to the bath should be small compared to the original level spacing. Our approach is therefore limited to the case of low damping. Several experiments[4-6] have been performed in this regime with a Q factor of 10 or larger. We shall see in the comparison of our solution to data that in most cases our approximation is adequate for explaining the results to within experimental uncertainties.

A complete set of states for a particle in the potential specified in Eq. (3.3) is the set of scattering states, since there are obviously no bound states. It is straightforward to integrate the Schrödinger equation numerically and examine the nature of these states. If one plots the phase shift of such states versus their energy one can readily identify resonances. These resonances are sharp for energies deep within the well; they broaden as the energy approaches the barrier top. There is always a broad resonance above the barrier top for the range of parameters relevant to the experiments[5,6] and beyond that a smoothly varying continuum. An alternative representation of these resonances are quasistationary states that have a long lifetime inside the metastable well. Around the nth resonance centered at energy E_n, the quasistationary state $\langle x \mid n \rangle = \Psi_n(x)$ is constructed out of a wave packet of scattering states $\varphi_E(x)$,

$$\Psi_n(x,t) = \int dE \, \chi_n(E) \varphi_E(x) e^{-iEt/\hbar} . \tag{3.5}$$

$\chi_n(E)$ will be centered around E_n with a spread given by the width of the nth state. At $t=0$, $\Psi_n(x,0)$ can be arranged to have a large amplitude inside the well by an appropriate superposition of the $\varphi_E(x)$'s around $E = E_n$. This is possible because for $E \simeq E_n$, $\varphi_E(x)$ changes very slowly with E within the well but undergoes rapid oscillation outside the well. Since there are many φ_E''s within the width of the smooth envelope χ, their amplitude will cancel outside the well. As time evolves, this initial alignment is gradually destroyed by the different energy components evolving at different rates. After a time of the order of the inverse of the energy width of $\chi_n(E)$, the particle will build up an appreciable weight outside the well and this time scale is defined to be the lifetime of the quasistationary state. A natural way to pick $\chi_n(E)$ is to identify it with the energy derivative of the phase shift around E_n which is approximately a Lorentzian with a full width at half maximum equal to the inverse lifetime of the state. Performing the energy integral in (3.5) then yields an exponentially decaying state with its wave function to the left of the barrier given by $\varphi_{E_n}(x)$. Its amplitude to the right of the barrier is assumed to be exponentially small. If one prepares an initial state by putting the particle inside such a well with very high barrier and then gradually lowering the barrier height (which is in fact the experimental situation), one would expect the state of the particle to be well-spanned by such quasistationary states as long as it remains inside the well. The authors of Ref. 8 suggested another way of obtaining some insight into the nature of the wave function of these quasistationary states by normalizing the scattering states φ_E in the continuum. Their analysis applies only to states near the barrier top and we will defer the discussion of such until we come across them naturally.

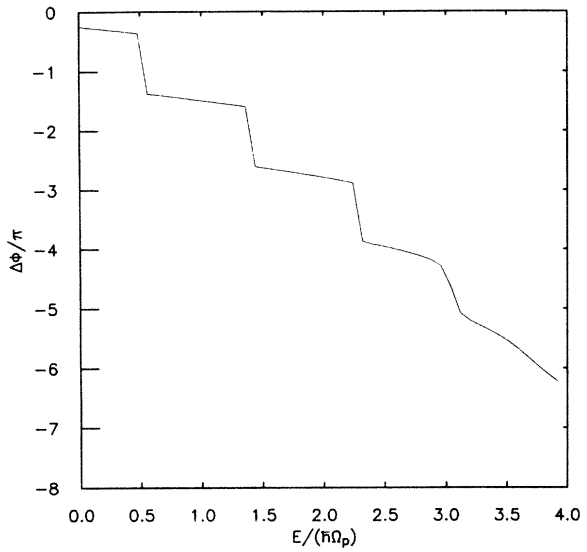

FIG. 2. Typical scan of phase shifts in units of π vs energy in units of $\hbar\Omega_p$. $U \simeq 3.054\hbar\Omega_p$ for this plot.

We now start with a discussion of the well-known semiclassical quantization rule for determining the level positions within a potential well. As our calculation is carried out mostly in regimes where there are only a few metastable states within the well, we performed a brute-force calculation to verify the accuracy of the semiclassical approximation. The energies of the resonances can be determined by numerically computing the phase shifts of the scattering states. A typical scan through the energy range is shown in Fig. 2. For the levels deep inside the well, we find that the level position is given to very good accuracy by the Born-Sommerfeld quantization rule employed in Ref. 8,

$$\oint p\,dq = 2\pi\hbar(n+\tfrac{1}{2}) . \tag{3.6}$$

For the metastable potential (3.3), the momentum p is given by

$$p(q) = m\dot{q} = \left[\frac{2}{m}[E - V(q)]\right]^{1/2} .$$

Following the notation of Ref. 8, we introduce the variable $X = q/q_0$. Then (3.6) can be rewritten as

$$(4mU)^{1/2} q X_{23}^2 X_{13}^{1/2} \int_0^1 dt \left[t(1-t)\left[1 - \frac{X_{23}}{X_{13}} t\right]\right]^{1/2} = \pi\hbar(n+\tfrac{1}{2}) , \tag{3.6'}$$

where $X_1 > X_2 > X_3$ are the three turning points at energy E_n:

$$X^3 - \tfrac{3}{2}X^2 + \frac{E_n}{2U} = 0 .$$

The criterion for applying such semiclassical method is that there be at least a few levels under the well; let us call that number N for future reference. For the case of even two levels inside the well, we find that the numerical implementation of (3.6') agrees with our phase-shift analysis to 2% for the ground state. [Born-Sommerfeld quantization is, of course, not suitable for finding the position of states near the barrier top. We shall discuss the calculation of parameters pertaining to the Nth and $(N+1)$th state after we have gone through the calculation of the lower states.] The error for the ground state reduced to $<0.5\%$ for the case $N=4$.

As suggested by Larkin and Ovchinnokov,[8] the level width or escape rate of the deep levels is well approximated by the semiclassical formula

$$\gamma_n = \frac{1}{T(E_n)} e^{-2S_E(E_n)/\hbar} . \tag{3.7}$$

$T(E_n) = 2\oint dx/\dot{x}$ is the period of classical motion at energy E_n. It comes in as the normalization of the semiclassical wave function inside the well. $S_E = \int_{X_2}^{X_1} p_E dq$ is the Euclidean action under the barrier. The corresponding formula in Ref. 8 has some additional correction terms to (3.7) which are of the order of 3% or smaller. Since we have completely left out the effect of dissipation, which is to reduce the escape rate, we feel that it is consistent to leave out such corrections. For the ground state, we have chosen to substitute in place of (3.7) the result of the zero-temperature instanton calculation including dissipation.[1] This improvement over the naive semiclassical result will be significant in the extreme quantum regime when the temperature is much lower that the typical level spacing.

We have checked the accuracy of (3.7) and the instanton result for the range of parameters relevant to experiment by taking the energy derivative of the phase shift and fitting it to a Lorentzian. The discrepancy ranges from a few percent for $N=4$ to the worst case of about 20% when N is barely two. Thus, the semiclassical approximation suffices until one can measure the absolute escape rate experimentally to better than a few percent.

Given the energy levels and therefore the semiclassical wave functions of the deep levels, we now proceed to calculate the corresponding $\{W_{k\to j}\}$ which give rise to bath-induced transitions between the resonance levels. According to the discussion in Sec. II, the equation of evolution for the entries of $\hat{\rho}$ are then

$$\dot{\hat{\rho}}_{jj} = \frac{1}{i\hbar}\langle j \,|\, [H_{\rm ext}, \hat{\rho}] \,|\, j\rangle + \sum_k W_{k\to j}\hat{\rho}_k - \sum_k W_{j\to k}\hat{\rho}_j - \gamma_j\hat{\rho}_j \tag{3.8a}$$

and

$$\dot{\hat{\rho}}_{jk} = \frac{1}{i\hbar}\langle j \,|\, [H_{\rm ext}, \hat{\rho}] \,|\, k\rangle - \tfrac{1}{2}(W_{j\to j+1} + W_{j\to j-1} + W_{k\to k+1} + W_{k\to k-1} + \gamma_j + \gamma_k)\hat{\rho}_{jk} . \tag{3.8b}$$

In our notation, which differs from that of Ref. 8 in that

our q twice their q and our mass is therefore $\frac{1}{4}$ of theirs, the transition rates are given by

$$W_{k\to j}=\frac{2}{\hbar}|\langle j|q|k\rangle|^2 J(|\omega_{jk}|)\{[1+n(\omega_{jk})]\Theta(\omega_{jk}) + n(\omega_{kj})\Theta(\omega_{jk})\} . \tag{3.9}$$

where $\omega_{jk}=E_j-E_k$. For clarity we have written out the downward and upward transitions separately.

$W_{k\to j}$ has the meaning of a thermal transition rate from the kth to the jth state. Since the phonon states are assumed to be occupied according to the Bose-Einstein distribution function, the thermal transition rates obey the Boltzmann-type relation $W_{k\to j}=W_{j\to k}e^{-E_{kj}/k_BT}$. In the weakly anharmonic approximation, the neighboring matrix elements of q are much larger than nonneighboring elements. We therefore keep only the neighboring transition elements, i.e., $W_{j\pm1\to j}$. The second- or higher-neighbor matrix elements of q are smaller but nonzero and we have to keep them in, say, calculating the microwave-induced ground to second excited-state transition. From the discussion in Sec. II as well as from (3.8b) we see that the off-diagonal elements of the reduced density matrix decay and are not excited much if they are not pumped effectively by $H_{\rm ext}$. We therefore keep only that class of off-diagonal elements that are nearly in resonance with the frequency of the applied perturbation.

The matrix elements of q between neighboring states can be computed semiclassically in the following manner:

$$\langle j|q|j-1\rangle=\frac{\int dq\,\Psi_j^\dagger(q)q\Psi_{j-1}(q)}{(\langle j|j\rangle\langle j-1|j-1\rangle)^{1/2}} . \tag{3.10}$$

If we take Ψ_j to be the (WKB) wave function and neglect the tail external to the well, (3.10) becomes the discrete Fourier transform of the classical trajectory $q(t)$ at frequency $\omega_{jj-1}=(E_j-E_{j-1})/\hbar$. We pick the normalization of the WKB wave functions to be

$$\langle j|j\rangle_{\rm WKB}=T_j/m .$$

Then

$$\begin{aligned}\langle j|q|j-1\rangle&=\frac{m}{(T_jT_{j-1})^{1/2}}\oint dq\frac{1}{P_j^{1/2}P_{j-1}^{1/2}}q \times e^{i\int(P_{j-1}-P_j)dq'/\hbar},\\ &\simeq\frac{\omega_j}{2\pi}\oint dq\frac{q}{\dot q_j^{1/2}\dot q_{j-1}^{1/2}}e^{-i\int\partial P/\partial E dq\,\omega_{jj-1}},\\ &=\frac{\omega_j}{2\pi}\oint dt\,q(t)e^{-i\omega_{jj-1}t} .\end{aligned} \tag{3.11}$$

It is possible to perform the transform in (3.11) exactly for the potential (3.3) if one is familiar with elliptic integrals and functions as are the authors of Ref. 8. One begins by inverting the relation

$$t=\int_{X_3}^{X}\frac{dx}{\dot x}=\left[\frac{6}{4\Omega_P^2}\right]^{1/2}\times\int_{X_3}^{X}\frac{dy}{[(y-X_3)(X_2-y)(X_1-y)]^{1/2}} \tag{3.12}$$

to express $X(t)$ as

$$X(t)=X_3+X_{23}\mathrm{sn}^2\left[t\Omega_p\left[\frac{X_{13}}{6}\right]^{1/2},k^2=\frac{X_{23}}{X_{13}}\right] ; \tag{3.13}$$

where $X_{ij}=X_i-X_j$. $X(t)$ in (3.13) is periodic with a period $T=2/\Omega_P\left[6/X_{13}\right]^{1/2}K(k^2)$. The transform (3.11) then amounts to doing the integral

$$\int_0^{2K}du\cos\left[\frac{\pi u}{K}\right][X_3+X_{23}\mathrm{sn}^2(u)] . \tag{3.14}$$

The trick is to notice that

$$\int^u sn^2v\,dv=\frac{1}{k^2}\left[\left[1-\frac{E(K)}{K}\right]u-Z(u)\right] .$$

Here sn is the elliptic function, $E(K)$ is the complete elliptic integral of the second kind, and $Z(K)$ is the ζ function which has a sine expansion in $\sin(n\pi u/K)$. Thus the integral (3.14) picks out the first component in the sine series and one arrives at (4.16) of Ref. 8,

$$\begin{aligned}\langle j|q|j-1\rangle&=\frac{q_0}{T_j}\oint\left\{X_3+X_{23}\mathrm{sn}^2\left[t\Omega_p\left[\frac{X_{13}}{6}\right]^{1/2}\right]\right\}dt\\ &=\frac{-\pi^2X_{23}q_0}{2k^2K(k^2)\sinh(\pi K'/K)} .\end{aligned} \tag{3.15}$$

This completes the calculation of all parameters in the master equation (3.8) for the deep levels.

When a resonance level is close to the barrier top, we can always locate its width and position by numerical phase-shift analysis. However, Larkin, and Ovchinnikov[8] suggested a very elegant way of achieving the same result by way of analytically approximating the wave function of such states. To the left and right of the barrier, it is reasonable to assume that the WKB (or semiclassical) wave function is a good approximation. In the vicinity of the barrier top, one can approximate the barrier with an inverted parabola and thus obtain the "exact" wave function as combinations of parabolic cylinder functions. The WKB wave functions are then connected by matching them to the parabolic cylinder functions expanded to the lowest nontrivial order in its energy measured from the barrier top. One thus arrives at an analytic expression for the scattering states in the continuum for energies close to the barrier top. The positions

and widths of the resonances can then be extracted by examining either the phase or amplitude of the wave function. The details of this exercise are presented in Appendix B.

The correct normalization of a state with its energy in the continuum is a delta function in energy. We therefore have to scale the wave function $\Psi(E)$ as derived in Appendix B with a normalization constant $\Psi^r(E)=N(E)\Psi(E)$ such that

$$\langle \Psi^r(E') \mid \Psi^r(E) \rangle = \delta(E'-E) \ . \tag{3.16}$$

The scaling function $N(E)$ is given by

$$\langle \Psi(E) \mid \Psi(E') \rangle = \int dq \{ A_1^* A_1 [\Psi_1^-(E')]^* \Psi_1^-(E) + B_1^* B_1 [\Psi_1^+(E')]^* \Psi_1^+(E) + \text{nonsingular terms} \}$$
$$\simeq \frac{2\pi}{m} \delta(E'-E) e^{-2\pi y} \left| 1 + \frac{\sqrt{2\pi}}{\Gamma(\frac{1}{2}+iy)} e^{[\pi y/2 + i6s/5 + 2iy\ln(6\sqrt{2s})]} \right|^2 = N^{-2} \delta(E'-E) \ . \tag{3.17}$$

The probability density of the state $\mid \Psi^r(E) \rangle$ to the left of the barrier is proportional to $N(E)^2$. Figure 3 is a typical plot of $N(E)^2$ versus E. The peaked structures clearly indicate the positions of the higher resonances. The energies and widths obtained by fitting Lorentzians to these peaks agree very well with our phase-shift analysis. In actual calculation we always used the former method because it is easier to implement and much more economical in terms of computer time. It is only for the purpose of understanding the accuracy of the former method that we compare the two and agreement of better than 1% is obtained until the number of levels inside the well goes below three. Larkin and Ovchinnokov[8] chose to fit a Lorentzian to the matrix element $\mid \langle j \mid q \mid \Psi^r(E) \rangle \mid^2$ which gave level widths that are consistently smaller than our method or phase-shift analysis. Since the level width of a metastable state should be a property of its wave function, we have chosen not to fit it to the matrix element of an arbitrary operator. This method hinges on the expansion in the small parameter $y=(E-U)/(\hbar\Omega_p)$; therefore it is used only for the resonances immediately above and below the barrier (the former being the "virtual state" of Ref. 8). Note that there is no fundamental difference between these last two states and the lower states. What the above analysis does is to provide an analytic formula for $\chi(E)$ in (3.5).

The thermal transition rate between the last two states [the Nth and the $(N+1)$th] are calculated by an incoherent integration over the transition rates to the continuum states.[8] The integrand in question is $W_{E\to N}$ where $W_{E\to N}$ is still given by (3.9). The matrix element of q is again approximated by its semiclassical value

$$\mid \langle E_N \mid q \mid E \rangle \mid^2 = \mid \langle E_N \mid q \mid \Psi^r(E) \rangle \mid^2$$
$$= \frac{N(E)^2}{\langle E_N \mid E_N \rangle_{\rm WKB}} \left| \frac{2q_0}{4m} \oint dt \, X(t) e^{i\delta E t/\hbar} \right|^{1/2} = \frac{N(E)^2}{\langle E_N \mid E_N \rangle_{\rm WKB}} \left| \frac{3\pi q_0 \delta E}{m\Omega_p^2 \sinh(\pi\delta E/\Omega_p)} \right|^2 , \tag{3.18}$$

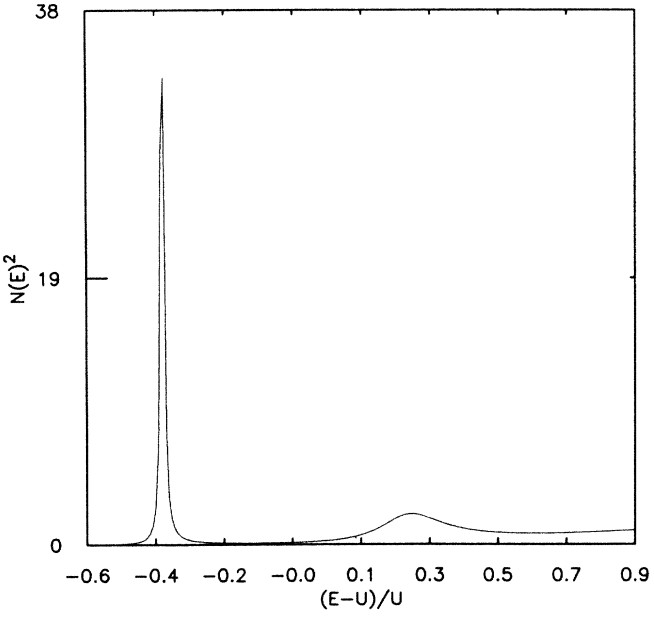

FIG. 3. Plot of $N(E)^2$ vs $(E-U)/U$ showing clearly the Nth and the much broader $(N+1)$th state. $U \simeq 3.544\hbar\Omega_p$ for this plot.

where the zero-temperature bounce $X(t) = 1 - \frac{3}{2}\cosh(\Omega_p t/2)^{-2}$ has been used. Note that in (3.18) we made the assumption that $\Psi_N(q) \simeq \langle q \mid E_N \rangle_{\rm WKB}$. The integration is carried over a window of energy centered around the energy level of the upper resonance. We picked this window such that the integration does not run into the neighboring resonances or that the integrand has dropped to $\frac{1}{200}$th of its peak value. In Ref. 8, it was indicated that the method of integrating over the continuum for the matrix element of q was also used for the $(N-1)$th to Nth transition. Our opinion is that the incoherent integration is an uncontrolled approximation and is to be avoided if possible. As long as the wave function is well localized within the well, one can opt to normalize the quasidiscrete state to one by cutting off the integration somewhere under the barrier. For the $(N+1)$th state, such a procedure is of dubious validity due to the large "tail" beyond the barrier, see Fig. 4. Therefore, one has to make the best approximation by integrating the analytical formula (3.18) over a carefully picked range of energy. For the $(N-1)$th to Nth transition, we have found that (3.15) gives a much better answer than integrating (3.18). We picked as the standard the matrix element

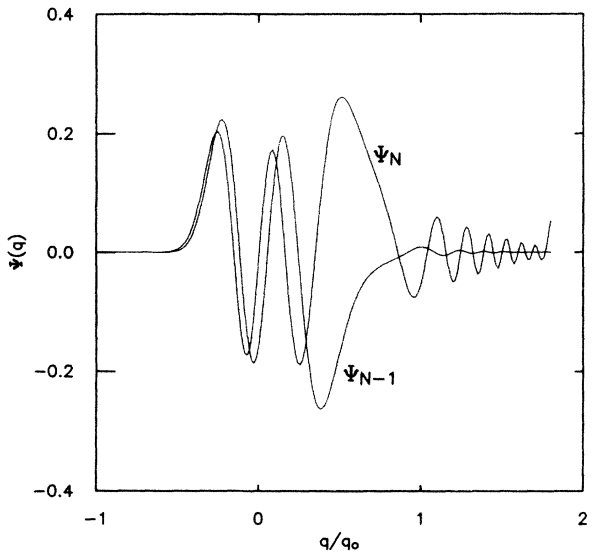

FIG. 4. Comparison of the amplitudes of the $(N-1)$th and the Nth state. The energy parameters are $U/(\hbar\Omega_p)\simeq 3.928$, $E_N/(\hbar\Omega_p)\simeq 3.920$, and $E_{N-1}/(\hbar\Omega_p)\simeq 3.206$. Note that the Nth state has a nontrivial tail beyond the barrier.

$\langle N \mid q \mid N-1 \rangle$ using numerical wave functions for both states. These wave functions are derived by starting with an exponential under the left barrier and integrating Schrödinger's equation outward. We found that q is very ineffective in coupling the two wave functions in the region outside the barrier until both of them have developed a substantial tail; i.e., our "standard" depends very weakly on where we chose to terminate the integration. Our calculation showed that, for the $(N-1)$th to Nth transition, (3.15) gave results that agreed with our standard to $\simeq 0.1\%$ while integrating (3.18) gave results that were too large by approximately 20%. This difference between our calculation and that in Ref. 8 will be important in the calculation of the ground to second excited-state resonance, see Sec. V.

In concluding this discussion of the semiclassical method, we note that it breaks down in the extreme quantum limit where there are only one to two levels within the well. In this regime, one can only resort to purely numerical methods, but the effect of dissipation is still poorly represented. Not only is one unable to include the effect of dissipation in the level widths but the thermal transition rates are also poorly calculated because the states, in general, are neither close to the barrier top nor deep inside the well.

Having obtained all the ingredients of the master equation (3.8a) and (3.8b), i.e., the level positions $\{E_j\}$, level widths $\{\gamma_j\}$, and thermal transition rates $\{W_{k\to j}\}$, we now discuss its solution. We search for a stationary solution for the diagonal elements of $\hat{\rho}$ by supplying a constant source at the well bottom.[18] This solution of the master equation will be a good approximation to the exact solution as long as the total escape rate from the well is small compared to the equilibrium rate within the well as determined by the $\{W_{k\to j}\}$. This condition is certainly satisfied for our parameters ranges where the total escape rate is $\lesssim 10^6\ \mathrm{s}^{-1}$ while the $W_{k\to j}$'s are of order GHz. We have also avoided the problem of choosing an initial condition for the reduced density matrix.

The set of equations (3.8) are homogeneous and therefore the only stationary solution is the trivial solution $\hat{\rho}_j \equiv 0$ unless we put in a source term. The source term C is put in at the equation for the ground state.

$$\dot{\hat{\rho}}_1 = 0 = W_{2\to 1}\hat{\rho}_2 - W_{1\to 2}\hat{\rho}_1 - \gamma_1\hat{\rho}_1 + (\text{microwave terms}) + C \ . \tag{3.19}$$

At this point, a simple example will serve to illustrate the general properties of the stationary solution of the master equation. Consider a two-state system in the absence of external perturbation where the escape rate of the lower state is negligible compared to all the other rates in the system. The components of the master equation are then

$$\begin{aligned} \frac{\partial\hat{\rho}_1}{\partial t} &= 0 = W_{2\to 1}\hat{\rho}_2 - W_{1\to 2}\hat{\rho}_1 + C \ , \\ \frac{\partial\hat{\rho}_2}{\partial t} &= 0 = W_{1\to 2}\hat{\rho}_1 - W_{2\to 1}\hat{\rho}_2 - \gamma_2\hat{\rho}_2 \ . \end{aligned} \tag{3.20}$$

Note that C is the current fed into the lower state which is in turn equal to the current leaking from the higher state $C=\gamma_2\hat{\rho}_2$. The normalized $(\hat{\rho}_1+\hat{\rho}_2=1)$ distribution gives an escape current

$$C = \frac{\gamma_2 e^{-E_2/k_BT}}{Z + \dfrac{\gamma_2}{W_{1\to 2}} e^{-E_2/k_BT}} = \begin{cases} \gamma_2\hat{\rho}_2^{\,\mathrm{eq}}, & \text{for } \dfrac{\gamma_2}{W_{1\to 2}} \to 0 \\ W_{1\to 2}, & \text{for } \dfrac{\gamma_2}{W_{1\to 2}} \to \infty \end{cases} , \tag{3.21}$$

where $Z = e^{-E_1/k_BT} + e^{-E_2/k_BT}$ and $\hat{\rho}_2^{\,\mathrm{eq}} = e^{-E_2/k_BT}/Z$ is the equilibrium Boltzmann distribution for the upper state. The solution in (3.21) shows clearly the "bottle neck" effect as one would expect it. If the upper state population is poorly replenished with a $W_{1\to 2}$ small compared with the depletion rate γ_2, the total escape current is basically the transition rate from the lower to the upper state. In the other extreme, if the leakage out of the upper state is slow, the distribution is close to equilibrium and the total current is just γ_2 times the equilibrium population of the upper state.

The only terms yet to be specified before we can solve (3.8), in general, are matrix elements of the form $\langle j \mid [H_{\mathrm{ext}},\hat{\rho}] \mid k \rangle$. We shall be concerned with two kinds of microwave perturbations. Their frequencies are such that we expect, (i) nearest-neighbor resonances $i\to i+1$ and, (ii) next-nearest-neighbor resonance $i\to i+2$. In the first case, the only off-diagonal matrix elements that are pumped effectively are the $\hat{\rho}_{j\,j\pm 1}$'s. According to the discussion in Sec. III, we therefore assume that only those off-diagonal elements are nonzero.

In the second case, we assume that only the $\hat{\rho}_{jj\pm2}$'s are nonzero. The next-nearest-neighbor matrix elements of $q, \langle j \mid q \mid j+2 \rangle$, can be calculated semiclassically along the same line of reasoning that led to (3.15). We simply quote the result here,

$$\langle j+1 \mid q \mid j-1 \rangle = \frac{-\pi^2 X_{23} q_0}{k^2 K(k^2) \sinh(2\pi K'/K)} . \quad (3.22)$$

One might view (3.22) with reasonable doubt when it is applied to a potential where the barrier height is around $4\hbar\omega_p$, the regime where experimental data are available. Surprisingly, when we checked (3.22) against the matrix element obtained from integrating numerical wave functions we consistently found agreement to one part in one thousand. Summarizing, the external perturbation term is given as

$$\langle j \mid [H_{\text{ext}}, \hat{\rho}] \mid j\pm1 \rangle = -\frac{I_1 \hbar}{2e} \cos(\bar{\omega} t) \langle j \mid q \mid j\pm1 \rangle (\hat{\rho}_{j\pm1 j\pm1} - \hat{\rho}_{jj}) , \quad (3.23)$$

for case (i), all other off-diagonal terms are set to zero. For case (ii),

$$\langle j \mid [H_{\text{ext}}, \hat{\rho}] \mid j\pm2 \rangle = -\frac{I_1 \hbar}{2e} \cos(\bar{\omega} t) \langle j \mid q \mid j\pm2 \rangle (\hat{\rho}_{j\pm2 j\pm2} - \hat{\rho}_{jj}) . \quad (3.24)$$

Again, all other off-diagonal terms are set to zero.

We assume that the potential is anharmonic enough that there is no degeneracy in the level spacing. This is a valid assumption in the limit of low damping since the resonances will be well resolved if their widths are small compared to their spacing. Given this assumption, the equation for the off-diagonal elements can then be readily solved by Fourier transform since the nondegeneracy assumption decouples the off-diagonal elements from each other. For example, when the microwave frequency $\bar{\omega}$ is such that we expect nearest-neighbor resonance,

$$\hat{\rho}_{j j+1} = -\frac{I_1}{4e} \frac{\langle j \mid q \mid j+1 \rangle (\hat{\rho}_j - \hat{\rho}_{j+1})}{(\bar{\omega} - \omega_{j+1} + \omega_j) - i\Gamma_j/2} e^{-i(\omega_{j+1} - \omega_j - \bar{\omega})t} , \quad (3.25)$$

where

$$\Gamma_j = \gamma_j + \gamma_{j+1} + W_{j\to j+1} + W_{j\to j-1} + W_{j+1\to j+2} + W_{j+1\to j}$$

and $\hat{\rho}_j$ is the population of level j. Substituting (3.25) into the equation for the diagonal elements, $\dot{\hat{\rho}}_j = 0$, gives (6.27) of Ref. 8:

$$\sum_k (W_{k\to j}\hat{\rho}_k - W_{j\to k}\hat{\rho}_j) - b_j W_{j+1\to j}(\hat{\rho}_j - \hat{\rho}_{j+1}) + b_{j-1} W_{j\to j-1}(\hat{\rho}_{j-1} - \hat{\rho}_j) - \gamma_j \hat{\rho}_j = 0 , \quad (3.26)$$

where

$$b_j = \frac{I_1^2}{16e^2} \frac{|\langle j \mid q \mid j+1 \rangle|^2}{W_{j+1\to j}} \frac{\Gamma_j}{(\bar{\omega} - \omega_{j+1} + \omega_j)^2 + \Gamma_j^2/4} . \quad (3.27)$$

When the microwave frequency is such that we expect next-nearest resonances, experimental data are available for the ground to second excited state and first to third excited-state resonance. The data correspond to a bias current range where there are four to five metastable states inside the well. Hence there are only three distinct microwave factors b_1, b_2, and b_3. They are distributed in the master equation as

$$\begin{aligned}
\dot{\hat{\rho}}_1 = 0 &= -(b_1 + W_{1\to2} + \gamma_1)\hat{\rho}_1 + W_{2\to1}\hat{\rho}_2 + b_1\hat{\rho}_3 + C , \\
\dot{\hat{\rho}}_2 = 0 &= W_{1\to2}\hat{\rho}_1 - (W_{2\to3} + W_{2\to1} + b_2 + \gamma_2)\hat{\rho}_2 + W_{3\to2}\hat{\rho}_3 + b_3\hat{\rho}_4 , \\
\dot{\hat{\rho}}_3 = 0 &= b_1\hat{\rho}_1 + W_{2\to3}\hat{\rho}_2 - (W_{3\to4} + W_{3\to2} + b_1 + b_3 + \gamma_3)\hat{\rho}_3 + W_{4\to3}\hat{\rho}_4 + b_3\hat{\rho}_5 , \\
\dot{\hat{\rho}}_4 = 0 &= b_2\hat{\rho}_2 + W_{3\to4}\hat{\rho}_3 - (W_{4\to5} + W_{4\to3} + b_2 + \gamma_4)\hat{\rho}_4 + W_{5\to4}\hat{\rho}_5 , \\
\dot{\hat{\rho}}_5 = 0 &= b_3\hat{\rho}_3 + W_{4\to5}\hat{\rho}_4 - (W_{5\to4} + b_3 + \gamma_5)\hat{\rho}_5 ,
\end{aligned} \quad (3.28)$$

where

$$b_i = \frac{I_1^2}{16e^2} |\langle i \mid q \mid i+2 \rangle|^2 \frac{\Gamma_i}{(\bar{\omega} - \omega_{i+2} + \omega_i)^2 + \Gamma_i^2/4} ,$$

$$\Gamma_i = W_{i\to i-1} + W_{i\to i+1} + W_{i+2\to i+1} + W_{i+2\to i+3} + \gamma_i + \gamma_{i+2} . \quad (3.29)$$

Here we have again substituted the relevant off-diagonal elements with the appropriate combination of diagonal elements similar to (3.25). Equations (3.26) and (3.28) are easily solved by inverting a matrix. The solution $\{\hat{\rho}_i\}$ is proportional to the feeding current C but the normalized total escape rate

$$\Gamma_{\text{tot}} = \frac{\sum_i \gamma_i \hat{\rho}_i}{\sum_i \hat{\rho}_i} \quad (3.30)$$

is independent of C. In Sec. V, we will compare the results of such calculations to experimental data.

IV. OHMIC AND NON-OHMIC DISSIPATIVE MECHANISMS

The origin of dissipation of Josephson junction is not completely well understood, but it is generally believed

that the classical behavior of the junction provides a prescription for determining the spectral density of the bath oscillators.[1,19] Within the resistively shunted junction (RSJ) model, the bath spectral function is given in terms of the junction capacitance C and shunt resistance R as

$$J(\omega)=m\gamma\omega\Theta(\omega_c-|\omega|)\,, \tag{4.1}$$

where the "mass" $m=(\hbar/2e)^2C$, and the damping coefficient $\gamma=1/RC$. Here ω_c is some high-frequency cutoff which is not necessarily as sharp as the step function which we have chosen here. The level shifts are approximately constant for all levels in the case of Ohmic dissipation because the junction provides a weakly anharmonic potential. [See the discussion following (2.20)]. Although a great deal of experimental ingenuity has been applied to measuring the "shunt" resistance of the junction, experiments with Ohmic dissipation have the problem that the junction parameters cannot be determined until the junction has been fabricated. It is therefore very difficult, if not impossible, to observe the effect of changing dissipation on the population distribution and escape rate.

There are experiments[10] in progress that allow the experimentalists to change the dissipation *in situ*. The experimental arrangement is basically a Josephson junction loaded with a transmission line of variable length l, see Fig. 5. The junction is characterized by the critical current I_c and capacitance C as before. It is loaded with a transmission line of characteristic impedance per unit length $Z_1^0=(L_1/C_1)^{1/2}$ which is a real number. This first transmission line is terminated with a second transmission line which has an absorptive medium such that the microwave signal fed in through the small capacitance c does not reach the end of the second line $A''B''$. The impedance at $A'B'$ is thus $Z_2(\omega)=Z_2^0$. The general form of the impedance at position x (as measured from AB) in line 1 is

$$Z_1(x)=Z_1^0\frac{R_1e^{+i\gamma_1x}+e^{-i\gamma_1x}}{R_1e^{+i\gamma_1x}-e^{-i\gamma_1x}}\,, \tag{4.2}$$

where R_1 is to be determined by boundary conditions and $\gamma_1=\omega/v_1$; v_1 being the speed of light along line 1.

Matching impedance at $A'B'$ then gives us the effective impedance loading the junction at AB,

$$Z_{\rm load}=Z_1^0\frac{Z_2^0-iZ_1^0\tan(\gamma_1l)}{Z_1^0-iZ_2^0\tan(\gamma_1l)}\,. \tag{4.3}$$

According to the prescription given by Leggett,[19] the spectral density $J(\omega)$ is then given by

$$J(\omega)=\left[\frac{\hbar}{2e}\right]^2\omega{\rm Re}\left[\frac{1}{Z_{\rm load}(\omega)}\right]\,. \tag{4.4}$$

This implies a more prominent frequency dependence for the $W_{k\to j}$ than given by (3.9). A much more dramatic differences compared with the Ohmic case arises from the nontrivial energy shifts. Assuming that the potential is nearly harmonic, the calculation of Sec. II for the energy shifts of a harmonic oscillator can be used, leading to

$$\delta E_n={\rm const}+\frac{n}{2}{\rm Im}\left[\frac{\hbar}{CZ_{\rm load}(\Omega_n)}\right]\,, \tag{4.5}$$

where $\hbar\Omega_n=E_{n+1}-E_n$. We have introduced the effect of the dissipation and level shifts (4.4) and (4.5) into the scheme of Sec. III to obtain some of the results given in Sec. V.

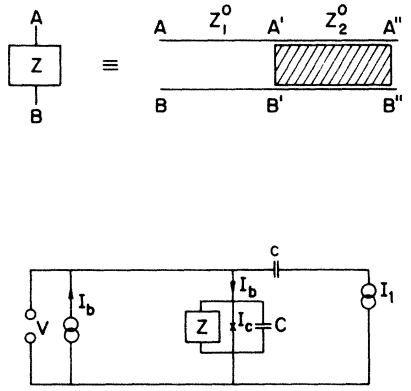

FIG. 5. Schematic diagram showing the experimental arrangement for a junction loaded with an absorptive transmission line (see Sec. IV). The small capacitance c couples the microwave current to the junction without causing any dc shift in the bias current.

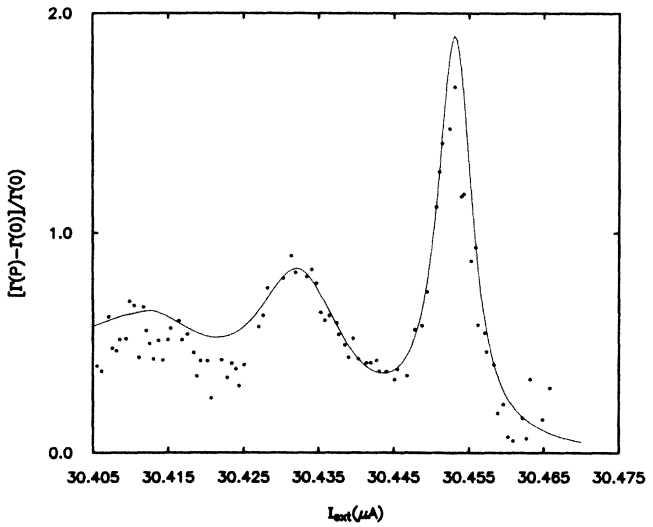

FIG. 6. Fit to the microwave enhancement data first published in Ref. 5. We used the exact parameters as supplied by the experimentalists; $I_c=30.572$ μA, $C=47$ pF, $R=134.7\Omega$ (as calculated from a Q of 80), $\bar{\omega}/2\pi=2.0$ GHz and a temperature of 28 mK. The fitting power P was 1.0×10^{-3}.

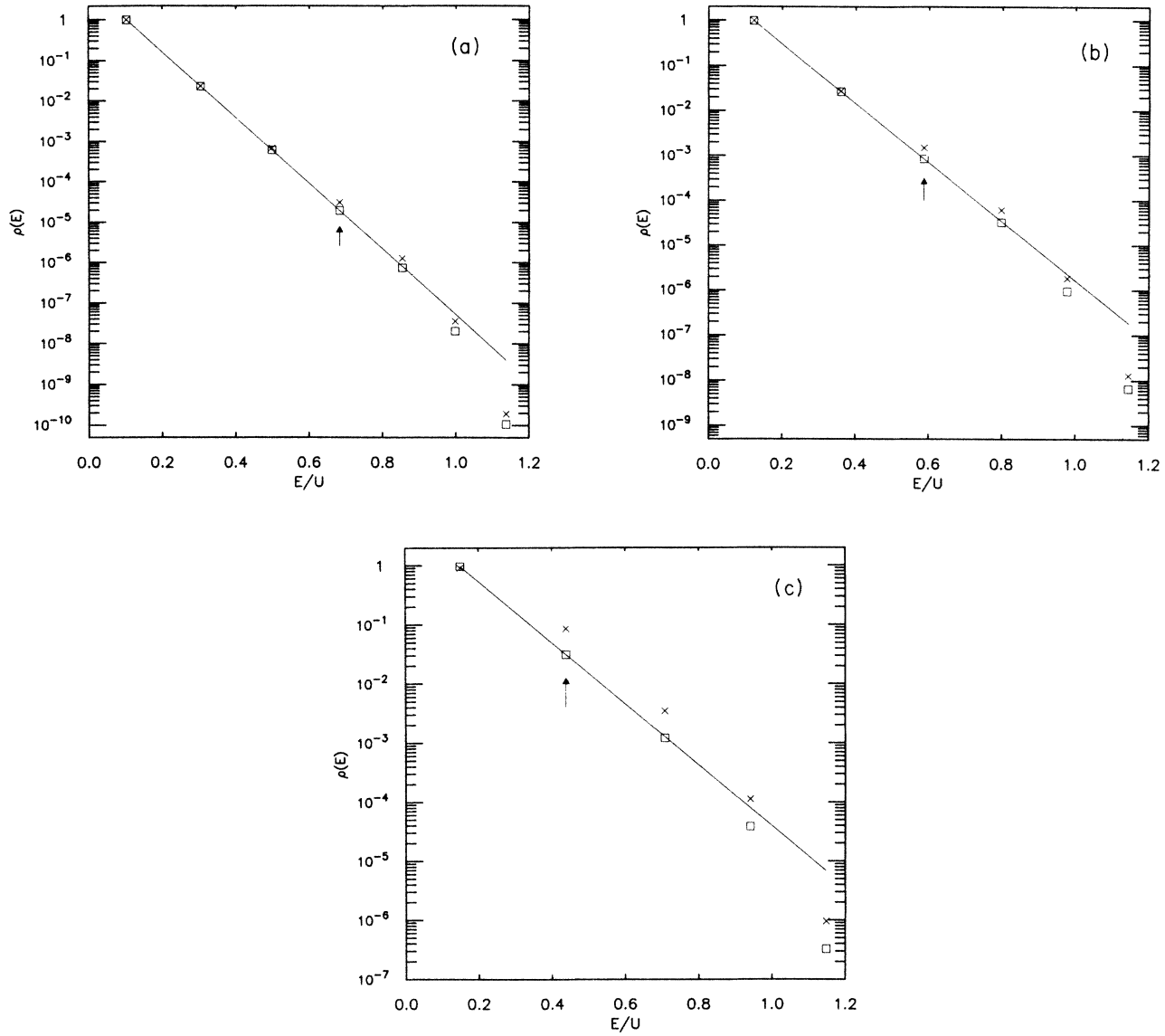

FIG. 7. (a) At the $2\rightarrow 3$ resonance as in Fig. 6, a plot of the normalized populations of all seven states ($N=6$). Naive Boltzmann distribution is shown as a straight line. The unenhanced populations according to Eq. (3.27) is shown as squares and the microwave enhanced populations as crosses. The level being pumped by the resonance is marked by the arrow. (b) Same as in (a) but for the $1\rightarrow 2$ resonance with six levels in all. (c) Same as in (b) but for the $0\rightarrow 1$ resonance with five levels in all.

V. CALCULATION AND RESULTS

In this section we present the results of our calculations. Figure 6 is a reproduction of the work of Ref. 8 and Figs. 7–12 are new results produced by our code. In comparing our calculations with published data, we have taken the liberty of shifting our curves along the current axis in order to achieve the best fit. Shifting the data along the current axis by a small amount is equivalent to changing the critical current by the same amount in the opposite direction. A small change in the critical current does not affect the calculation qualitatively but only gives the results a constant shift. The magnitude of this shift, however, is always small and well within the limits set by the uncertainties of the measured junction parameters.

Figure 6 is a fit to the microwave enhancement

$$\frac{[\Gamma_{\rm tot}(P\neq 0)-\Gamma_{\rm tot}(P=0)]}{\Gamma_{\rm tot}(P=0)}$$

versus bias current data as in Fig. 2 of Ref. 5. The junction parameters used are $I_c=30.572$ μA, $C=47$ pF, and $R=134.66\Omega$. The data have been given a constant current shift of 0.018 μA which is within the experimental uncertainty (the combined effect of δI_c and δC) as shown in Fig. 2(b) of Ref. 5. The only unmeasured parameter is the microwave power where following Larkin and Ovchinnikov, we define the dimensionless power P for a junction as

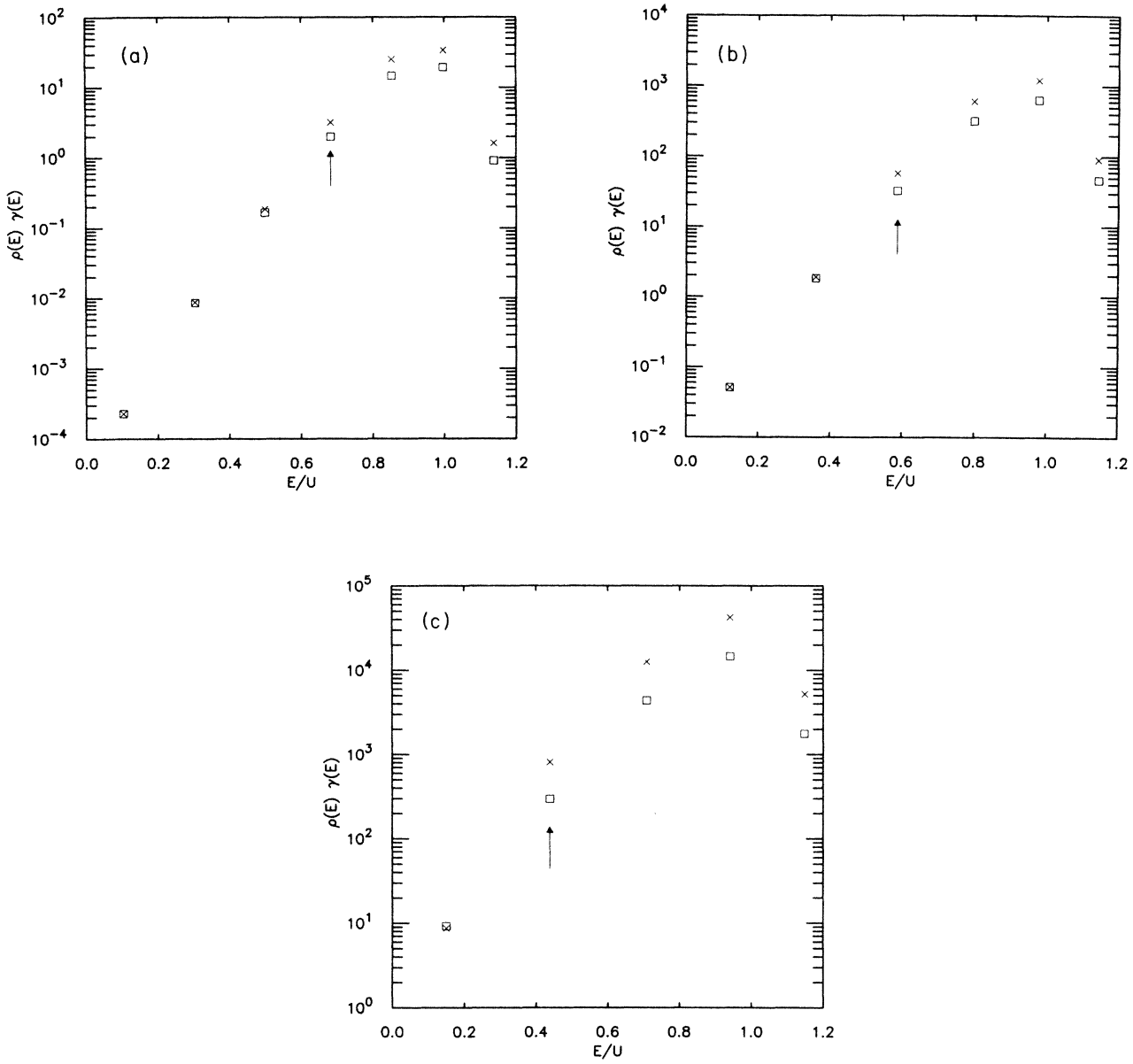

FIG. 8. Plot of $\hat{\rho}_i\gamma_i$ vs E_i/U with the same junction parameters as in Fig. 6. (a) The bias current is the same as in Fig. 7(a) which is at the $2\rightarrow 3$ resonance. Unenhanced escape currents are represented as squares and microwave enhanced currents as crosses. The level being pumped is marked by the arrow. (b) Same as (a) but at the $1\rightarrow 2$ resonance. (c) Same as (a) but at the $0\rightarrow 1$ resonance.

$$P\hbar\bar{\omega}^2=\tfrac{1}{2}\mathrm{Re}\left[\frac{1}{Z_{\mathrm{load}}(\bar{\omega})}\right]I_1^2 . \tag{5.1}$$

Our curve was produced with a P of 1×10^{-3}. The differences in the power used in our calculation and that of Ref. 8 ($P=8.57\times10^{-3}$) is probably due to the differences in the details of the calculation; the main one being the method of computing the thermal transition rate involving the last two states under the barrier. The separations, widths and relative heights of the three resonances agree very well with the calculation. Figures 7 and 8 serve to provide some insights into the inner workings of the calculation that led to Fig. 6. Figures 7(a)–7(c) are plots of the normalized populations $\{\hat{\rho}_i\}$ for three values of the bias current corresponding to a resonance for the $2\rightarrow3$, $1\rightarrow2$, and $0\rightarrow1$ transitions, respectively. The naive Boltzmann distribution is shown as a straight line, and the actual population in the absence and presence of microwave are shown as squares and crosses, respectively. We see that deep inside the well, the distribution is almost Boltzmannian, since the escape rates of these states are small. Microwave pumping enhances the population of all states above the resonance while the populations of the last two states are al-

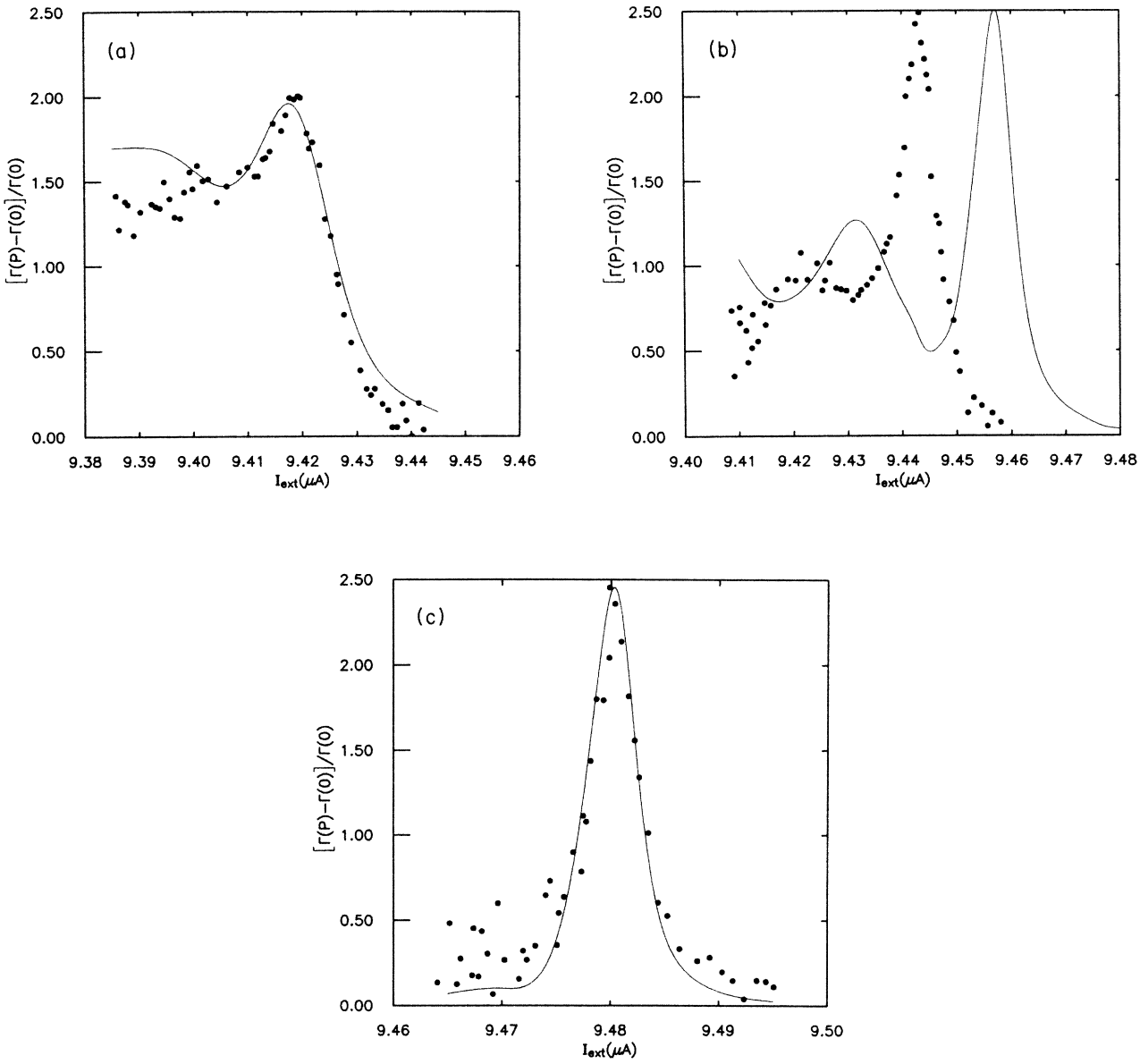

FIG. 9. Fits to microwave enhancement of escape rate data presented in Fig. 20 of Ref. 11. We used $I_c = 9.5715\ \mu A$, $C = 5.95$ pF, and $R = 350\ \Omega$ for the junction parameters. Other parameters are (a) $T = 97.19$ mK, $\bar{\omega}/2\pi = 4.5$ GHz, and power $P = 7.7 \times 10^{-3}$; (b) $T = 57.06$ mK, $\bar{\omega}/2\pi = 4.1$ GHz, and power $P = 2.1 \times 10^{-3}$; (c) $T = 17.76$ mK, $\bar{\omega}/2\pi = 3.7$ GHz, and power $P = 1.54 \times 10^{-4}$.

ways lower than the Boltzmann distribution due to depletion by significant leakage. This serves to demonstrate a weakness in the "finite temperature instanton"[20-22] method of calculating escape rates which assumes that all levels are populated according to the Boltzmann distribution. Figures 8(a)–8(c) show the contribution of the individual states to the total escape rate Γ_{tot} as in (3.30). The biggest contribution is always from the state just below the barrier top with or without applied microwaves. This is in line with expectation, since the junction temperature is about twice the crossover temperature.[20-22] The contribution of the virtual state is reduced by the effect of depletion; the ratio $\gamma_{N+1}/W_{N\to N+1} \geq 50$ for all cases we have encountered. Any resonances beyond that would be so depleted that their contributions would be negligible.

To demonstrate the effect of temperature, we have performed calculations for another junction with $I_c = 9.5715\ \mu A$ and $C = 5.95$ pF.[5,11] These fits to the data in Figs. 9(a)–9(c) are obtained by varying the capacitance until the current spacing between the 4.5-GHz peak and the 3.7-GHz peak agrees with the data and then shifting all three calculated curves along the current axis by varying I_c. Note that the capacitance used is still within the experimental uncertainty of the measured value and we have picked a shunt resistance of

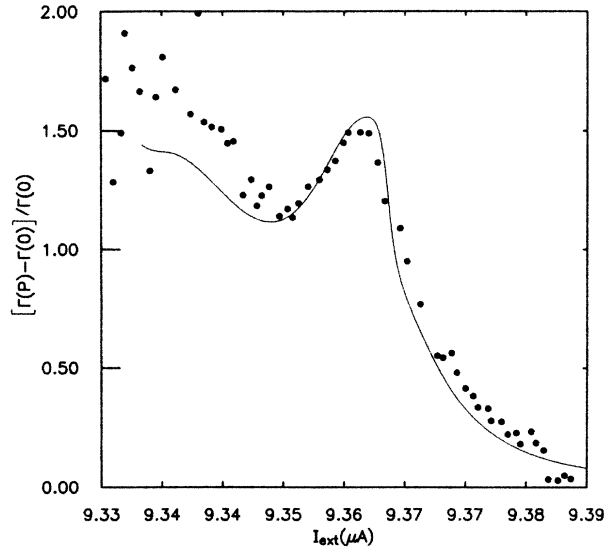

FIG. 10. Fit to microwave enhancement data for the $0\rightarrow 2$ and $1\rightarrow 3$ resonances in Fig. 19 of Ref. 11. Junction parameters used are $I_c=9.489$ μA, $C=6.35$ pF, and $R=120$ Ω. Other parameters are $T=57$ mK, $\bar{\omega}/2\pi=7.9$ GHz, and power $P=1.0\times 10^{-2}$.

350 Ω to obtain the right line shape. The value of the resistance used is significantly higher than the 190 ± 100 Ω quoted in Ref. 11 but we would like to point out that Martinis *et al.*, were concerned with establishing a lower bound to the resistance. For example, for a Q value of 30 (which is the correct value for the particular junction), Table I of Ref. 11 indicated that the shunt resistance should be 50% higher than the conservative

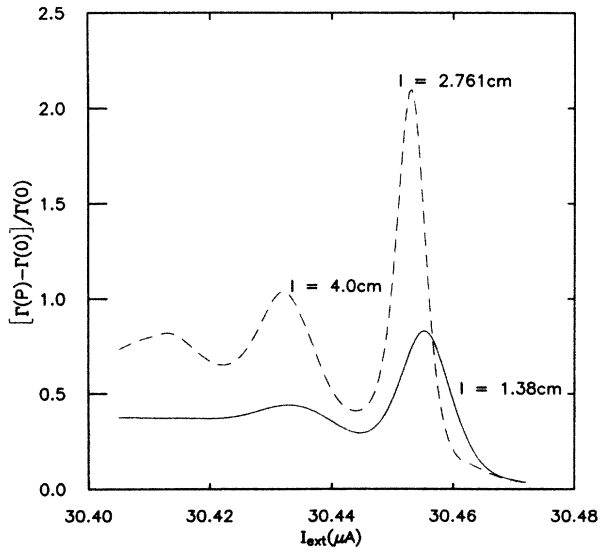

FIG. 11. Microwave enhancement vs bias current for a transmission line loaded junction with the same parameters as in Fig. 6. The line impedances chosen were $Z_1^0=75$ Ω, $Z_2^0=Z_1^0/2$, and $v_1=2.22\times 10^{+8}$ m/s. l is the length of the transmission line 1. The microwave power used was the same in all three cases, $P=1.0\times 10^{-3}$.

estimate that gave 190Ω, thus bringing the theoretical and experimental value within the uncertainty of the latter. We have not been able to put all three calculated peaks on top of the experiment ones but their line shapes all agree beautifully. The discrepancy in the peak positions amounts to an error in the calculated level spacing of about 4%, not much higher than our expected accuracy for the semiclassical method in the quantum regime. The same junction has been used to obtain data for the $0\rightarrow 2$ and $1\rightarrow 3$ resonance. Figure 10 shows our fit to the data taken from Ref. 11. In addition to using a slightly lower critical current as explained by the experimentalists, we found that a lower shunt resistance of 120 Ω gives a much better fit to the data. This frequency-dependent dissipation actually agrees very well with the structure seen in the data, see Figs. 7 and 12 of Ref. 11. The overall shift along the current axis was 0.005 μA, which one might attribute to a frequency-dependent Lamb shift. Since the experimental uncertainty in the critical current is significantly larger than this shift, we have not attempted to calculate and compare the two.

Figure 11 shows the result of calculation of microwave enhancement of escape rate assuming a transmission line loading, see Sec. IV for details. We have used the same junction parameters as in Fig. 6 with the temperature set at 28 mK. We expect to be able to fit experimental data as soon as they become available. In Fig. 11, we try to demonstrate the effect of frequency-dependent Lamb shifts on such a microwave enhancement experiment. From Eq. (4.3) and (4.5), the interesting part of the frequency shift due to a transmission line loading is

$$\delta E_n \propto \frac{\sin(2\Omega_n l/v_1)}{5-3\cos(2\Omega_n l/v_1)}\ , \tag{5.2}$$

where l is the length of the transmission line 1 and v_1 is the speed of light along line 1. The three values of l chosen correspond to the $\sin(2\Omega_n l/v_1)$ factor being approximately $-1(l=4$ cm), $0(l=2.761$ cm), and $+1(l=1.38$ cm). We have assumed $Z_1^0=75$ $\Omega=2Z_2^0$ and a v_1 of 2.22×10^8 m/s. The frequency-dependent shifts are clearly observable and the power has been kept constant such that minimum dissipation (zero shift) corresponds to the sharpest resonance.

Figures 12(a)–12(c) are comparisons of the calculated versus measured escape temperature defined as[11]

$$\Gamma_{\rm tot}=\frac{\Omega_p}{2\pi}e^{-U/k_BT}\ . \tag{5.3}$$

The data have been presented in its original form without any shift in the current because shifting does not improve the fit by very much on the scale of this figure. The dotted lines are the upper and lower bounds of the calculated escape temperature due to experimental uncertainties in the critical current, junction temperature, and capacitance. The discrepancy demonstrated the biggest weakness of our calculation, i.e., the omission of the effect of dissipation on the escape rate of the individual states. As a result, our calculated escape rate, and thus the escape temperature, is higher than the measured value (except in the extreme quantum limit) although the

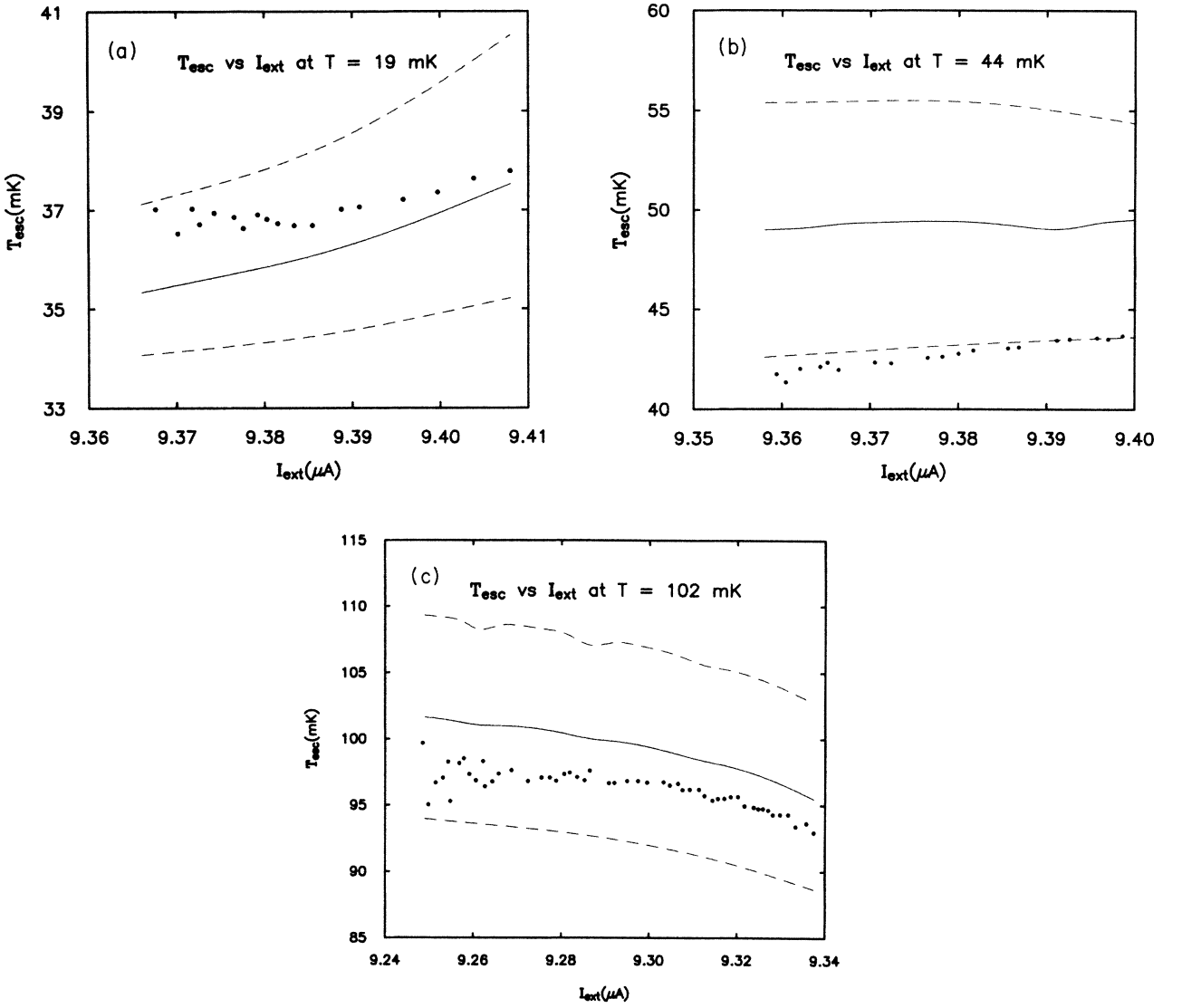

FIG. 12. Calculated vs measured T_{esc} for three different temperatures for the junction used in Fig. 10. The data are shown in dots and the calculated T_{esc} in solid lines. The dotted lines are the upper and lower bounds to the calculated T_{esc} allowed by the uncertainties in the junction temperature, capacitance, and critical current.

general trend is in agreement. The microwave enhancement calculation is not so sensitive to the absolute value of the level widths because the line shape depends more on the thermal transition elements, and because the microwave power is fitting parameter. In the regime of our calculation, where the ratio $\Delta U/\hbar\Omega_p$ is never very large, we are not aware of any theoretical prediction of the effect of dissipation on the escape rate of the excited states. We think this is an area that deserves further theoretical investigation.

ACKNOWLEDGMENTS

We thank A. I. Larkin and Yu. N. Ovchinnikov for providing us with a copy of their work prior to publication, and the latter for explanations of parts of this work. We are also grateful to A. Cleland, M. Devoret, S. Hershfield, J. Martinis, and A. Schmid for helpful discussions. This work was supported by the National Science Foundation under Grant No. DMR-84-17555

APPENDIX A

In this Appendix we will outline a proof that $\hat{G}(\omega)=\exp(-\beta\omega)A(\omega)$ is a general result in equilibrium. We will do this by first analyzing the self-energy corrections for G^r and $\hat{G}$ to learn the Feynman rules. Then we will consider one fourth-order correction to the self-energy which is sufficiently complicated that all the general features of the nth-order diagrams can be seen. It will also give an opportunity to examine how the di-

agrammatic technique is used in this formalism.

In the text it was mentioned that the Nth-order terms can be found by expanding out the time evolution operators and taking the resulting trace over the bath degrees of freedom. Let us see this in more detail.

In the following we will ignore the counterterm, so the interaction term is given by $V_I(t)=-F(t)q(t)$, where $F(t)=\sum_i C_i x_i(t)$ operates on the bath coordinates and $q(t)$ operates on the particle. The Nth order term to $\hat{G}(t,t')$ is given by a sum of $(2N+1)$ terms that come from expanding $U(t,t_0)$ to kth order and $U^\dagger(t_0,t')$ to $(N-k)$th order, where k runs from 0 to N:

$$\sum_{k=0}^{N}(-i)^k(i)^{N-k}\int d\tau_1\int d\tau_2\cdots\int d\tau_N e^{-iH_0 t}\mathrm{Tr}_{\mathrm{bath}}[V_I(\tau_1)V_I(\tau_2)\cdots V_I(\tau_k)e^{iH_0 t_0}\hat{\rho}(t_0)\rho_{\mathrm{eq}}^{\mathrm{bath}} \times e^{-iH_0 t_0}V_I(\tau_N)\cdots V_I(\tau_{k+1})]e^{-iH_0 t'}, \tag{A1}$$

where the integrals are over $t>\tau_1>\tau_2>\cdots>\tau_k>t_0$ and $t'>\tau_{k+1}>\cdots>\tau_N>t_0$. Since the density matrix at the initial time, which we will assume was in the distant past, is of the Feynman-Vernon form of a product of a density matrix for the particle times one for the bath, the terms acting on the particle can be removed and the problem reduces to calculating

$$\sum_{k=0}^{N}(-i)^k(i)^{N-k}\int d\tau_1\int d\tau_2\cdots\int d\tau_N\mathrm{Tr}_{\mathrm{bath}}[F(\tau_1)\cdots F(\tau_k)\rho_{\mathrm{eq}}^{\mathrm{bath}}F(\tau_N)\cdots F(\tau_{k+1})] \times e^{-iH_0 t}q(\tau_1)\cdots q(\tau_k)e^{iH_0 t_0}\hat{\rho}(t_0)e^{-iH_0 t_0}q(\tau_N)\cdots q(\tau_{k+1})e^{+iH_0 t'}. \tag{A2}$$

The product of q's is in the interaction representation which can be written in a simple form by removing the factors $\exp(\pm iH_0\tau)$ multiplying q. If we then take note of the domain of integration that the time-ordering imposes, and define the bare retarded and advanced Green functions by Eq. (2.8), the product of q's can be written as

$$G_0^r(t-\tau_1)qG_0^r(\tau_1-\tau_2)q\cdots qG_0^r(\tau_k-t_0)\hat{\rho}(t_0)G_0^a(t_0-\tau_N)qG_0^a(\tau_N-\tau_{N-1})q\cdots qG_0^a(\tau_{k+1}-t'). \tag{A3}$$

It should be noted that the Nth order term of the full retarded Green function can also be written as a string of G's and q's but the Green's functions are all retarded. Similarly, the advanced Green function produces a string of all advanced Green functions in time-reversed order. These strings of G's are multiplied by this bath correlation function at $2N$ times. Since the bath is described as a set of harmonic oscillators and coupling between the bath and the particle is linear in the bath coordinate the correlation function breaks up into a sum over all possible partitions of the $(2N)F(\tau)$'s into pairs. There is only one subtlety in the process. If the two τ's lie both to the right or both to the left, then the time arguments of the correlation can be gotten by putting the one on the left first. If, however, one is to the right and one is to the left, it is the leftmost time argument that goes last. Specifically,

$$\begin{aligned}&\mathrm{Tr}_{\mathrm{bath}}[F(\tau_i)F(\tau_j)\rho_{\mathrm{eq}}^{\mathrm{bath}}]=\alpha(\tau_i-\tau_j),\\ &\mathrm{Tr}_{\mathrm{bath}}[F(\tau_i)\rho_{\mathrm{eq}}^{\mathrm{bath}}F(\tau_j)]=\alpha(\tau_j-\tau_i),\\ &\mathrm{Tr}_{\mathrm{bath}}[\rho_{\mathrm{eq}}^{\mathrm{bath}}F(\tau)_iF(\tau_j)]=\alpha(\tau_i-\tau_j),\end{aligned} \tag{A4}$$

where

$$\alpha(\tau)=\int_{-\infty}^{\infty}\frac{d\omega}{2\pi}J(\omega)[1+n(\omega)]e^{-i\omega\tau}. \tag{A5}$$

In fact, the above result is a simple consequence of the cyclic property of the trace, but it is the mathematical source of the equilibrium condition we seek to show.

To write out the diagrams, we write a G_0^r as a directed line segment pointing to the left, a G_0^a as a line segment directed to the right and $\hat{G}_0$ as a line segment with a circle on it [representing the $\hat{\rho}(t_0)$] with arrows at both ends. This notation was chosen since the noninteracting $\hat{G}_0(t,t')$ is given by

$$\hat{G}_0(t,t')=G_0^r(t,t_0)\hat{\rho}(t_0)G_0^a(t_0,t').$$

The particle-bath vertex gives a value q between two G's.

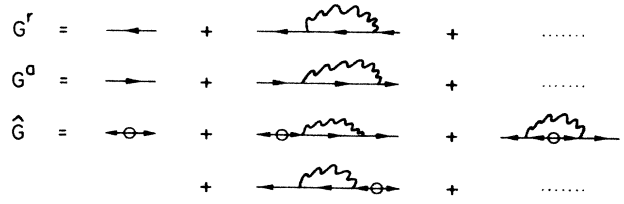

FIG. 13. The lowest-order corrections to the Green functions. Note that the corrections for $\hat{G}$ can be derived from those of G^r by replacing one of the G_0^r with a $\hat{G}_0$ and reversing all the arrows to the right of it.

The bath propagator, represented as a wiggly line, has the order of its time arguments reversed if it spans the $\hat{G}_0$. The lowest-order Feynman diagrams for the Green's functions are shown in Fig. 13. Notice that the corrections to $\hat{G}$ can be derived from the corrections to G^r by replacing in all possible ways one of the G_0^r's with a $\hat{G}_0$ and changing all the G_0^r's to the right of it into G_0^a's.

We will now set out to prove our relation $\hat{G}(\omega) = \exp(-\beta\omega)A(\omega)$. We will examine the contribution in Fig. 14(a) to G^r. The corresponding self-energy for G^a is given by reversing all the arrows. For this particular term, there will be five corresponding terms in $\hat{G}$ depending on which internal line the $\hat{\rho}$ factor is inserted. These are shown in Fig. 14(b). Consider now the contribution of 14(a) to the spectral function $A(\omega)=i[G^r(\omega)-G^a(\omega)]$. It is given by

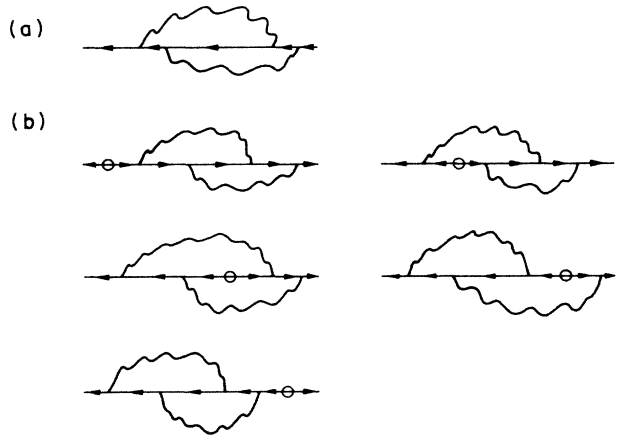

FIG. 14. (a) Fourth-order correction to G^r. (b) The five corrections to $\hat{G}$ which can be uniquely derived from (a).

$$\delta A(\omega)=i\int d\omega'\int d\omega''\alpha(\omega')\alpha(\omega'')[G_0^r(\omega)qG_0^r(\omega-\omega')qG_0^r(\omega-\omega'-\omega'')qG_0^r(\omega-\omega'')qG_0^r(\omega) - G_0^a(\omega)qG_0^a(\omega-\omega')qG_0^a(\omega-\omega'-\omega'')qG_0^a(\omega-\omega'')qG_0^a(\omega)] \tag{A6}$$

which equals

$$\begin{aligned}\delta A(\omega)=\int d\omega'\int d\omega''\alpha(\omega')\alpha(\omega'')[&A(\omega)qG_0^a(\omega-\omega')qG_0^a(\omega-\omega'-\omega'')qG_0^a(\omega-\omega'')qG_0^a(\omega)\\ &+G_0^r(\omega)qA(\omega-\omega')qG_0^a(\omega-\omega'-\omega'')qG_0^a(\omega-\omega'')qG_0^a(\omega)\\ &+G_0^r(\omega)qG_0^r(\omega-\omega')qA(\omega-\omega'-\omega'')qG_0^a(\omega-\omega'')qG_0^a(\omega)\\ &+G_0^r(\omega)qG_0^r(\omega-\omega')qG_0^r(\omega-\omega'-\omega'')qA(\omega-\omega'')qG_0^a(\omega)\\ &+G_0^r(\omega)qG_0^r(\omega-\omega')qG_0^r(\omega-\omega'-\omega'')qG_0^r(\omega-\omega'')qA(\omega)]\ .\end{aligned} \tag{A7}$$

If we write down from Fig. 14(b) the corresponding five expressions for the term in $\hat{G}$, we find exactly the same kind of structure except that the $\alpha(\omega)$ are replaced by $\alpha(-\omega)$ if they bridge the $\hat{\rho}(t_0)$ factor. If we use the identity $\alpha(-\omega)=\exp(-\beta\omega)\alpha(\omega)$ we find that the expression for $\hat{G}$ is identical to (A7) above except for an overall factor of $\exp(-\beta\omega)$, as we set out to show.

APPENDIX B

In this Appendix we will describe in some details the calculation of the semiclassical wave function for energies close to the barrier top. This is meant to be a supplement to the terse outline given in Ref. 8.

In the classically forbidden region 3, see Fig. 1, the wave function is a decaying exponential

$$\Psi_3(E)\simeq\frac{1}{\sqrt{k}}e^{-q_0\int_x^{X_3}k\,dx}, \tag{B1}$$

where

$$k=\left[\frac{4mU}{\hbar^2}\right]^{1/2}[(X_3-x)(X_2-x)(X_1-x)]^{1/2}\ .$$

Ψ_3 continued into the well becomes a standing wave which in the semiclassical approximation is

$$\Psi_2(E)=\frac{2}{\sqrt{k}}\cos\left[q_0\int_{X_3}^{X}k\,dx-\frac{\pi}{4}\right]\ . \tag{B2}$$

Here

$$k=\left[\frac{4mU}{\hbar^2}\right]^{1/2}[(x-X_3)(X_2-x)(X_1-x)]^{1/2}\ .$$

For the purpose of matching, we need to expand the phase in (B2) for X close to the turning point X_2 but not so close that the semiclassical approximation fails. We shall define the parameters of expansion to be $\delta x=(X_1+X_2)/2-X$ and $\Delta=X_{12}$. After a bit of tedious algebra one emerges with the expression

$$q_0 \int_{X_3}^{X} k\,dx = q_0 \left[\frac{4mU}{\hbar^2}\right]^{1/2} X_{23}^2 X_{13}^{1/2} \left[\frac{\pi}{8} F\left(-\frac{1}{2},\frac{3}{2},3,\frac{X_{23}}{X_{13}}\right) - \frac{2\delta X^2}{9} + \frac{1}{2}\left[\frac{\Delta}{3}\right]^2 \ln\left[\frac{4\,|\,\delta x\,|}{\Delta}\right] + \frac{\Delta^2}{36}\right] . \tag{B3}$$

Here $F(-\frac{1}{2},\frac{3}{2},3,X_{23}/X_{13})$ is a hypergeometric function.

Beyond the barrier, the wave function is a superposition of an incoming and outgoing wave of equal weight (such that probability is conserved). These two waves are again given in the semiclassical approximation by,

$$\Psi_1^{\pm} \simeq \frac{1}{\sqrt{k}} e^{\pm i \int^X k\,dx} . \tag{B4}$$

In this region, the phase in (B4) can be expanded in terms of the energy as measured form the barrier top as

$$\begin{aligned}\int^X k\,dx &= q_0 \left[\frac{4mU}{\hbar^2}\right]^{1/2} \\ &\quad \times \int^X [x-X_3)(x-X_2)(x-X_1)]^{1/2} dx , \\ &\simeq \left[\frac{6mU}{\hbar^2}\right]^{1/2} \int^X [(x-X_2)(x-X_1)]^{1/2} dx , \\ &\simeq s\left[\frac{\delta x^2}{2}\left[1-\frac{\Delta^2}{8\delta x^2}\right] - \frac{\Delta^2}{8}\ln\left[\frac{4\,|\,\delta x\,|}{\Delta}\right]\right] ,\end{aligned} \tag{B5}$$

where we have followed the notation of Ref. 8 with

$$s = q_0\sqrt{6mU} = m\Omega_p q_0^2 ,$$
$$y = \frac{E-U}{\hbar\Omega_p} .$$

y is the dimensionless expansion parameter which in turn is related to another small parameter $\Delta = X_{12}$ by $y = -s\Delta^2/8$. The final form of Ψ_1 that will be used for matching is

$$\Psi_1^{\pm} = \left[\frac{q_0}{s\delta x}\right]^{1/2} e^{\pm s\delta x^2 i/2} \left[\frac{4\delta x}{\Delta}\right]^{\pm iy} e^{\mp yi/2} . \tag{B4'}$$

In region 2 around the barrier top, Schrödinger's equation

$$-\frac{\hbar^2}{2mq_0^2}\frac{\partial^2\psi}{\partial X^2} + [3U(X^2 - \tfrac{2}{3}X^3) - E]\psi = 0 , \tag{B6}$$

can be transformed to the equation for the parabolic cylinder function by a change of variable $z = \sqrt{s}\,(X-1)$ and dropping the anharmonic term in z^3,

$$\frac{\partial^2\psi}{\partial z^2} + 2y\psi + z^2\psi = 0 . \tag{B7}$$

z is the appropriate variable for matching since it is equal to $(X_1+X_2)/2$ up to order Δ^2. For z large and negative and $\nu = -(\frac{1}{2}+iy)$, the solutions to (B7) have the asymptotic expansions

$$\begin{aligned} D_\nu^+(e^{-3\pi i/4}\sqrt{2}\,|\,z\,|) &\simeq e^{-z^2/2} e^{-3\pi i/2} (e^{-3\pi i/4}\sqrt{2}\,|\,z\,|)^\nu \\ &\quad - \frac{\sqrt{2\pi}}{\Gamma(-\nu)} e^{-\nu\pi i} e^{z^2/2} e^{-3\pi i/2} \\ &\quad \times (e^{-3\pi i/4}\sqrt{2}\,|\,z\,|)^{-1-\nu} \\ D_\nu^-(e^{\pi i/4}\sqrt{2}\,|\,z\,|) &\simeq e^{-z^2/2} e^{\pi i/2} (e^{\pi i/4}\sqrt{2}\,|\,z\,|)^\nu , \end{aligned} \tag{B8}$$

where $\Gamma(-\nu)$ is the gamma function of complex argument $-\nu$.

In order to match (B2) to (B8), we expand the phase of Ψ_2 as given by (B3) to order Δ^2 to obtain

$$\Psi_2 \simeq \left[\frac{q_0}{2\delta x}\right]\left[e^{i\theta} e^{-s\delta x^2 i/2}\left[\frac{4\delta x}{\Delta}\right]^{-iy} + e^{-i\theta} e^{s\delta x^2 i/2}\left[\frac{4\delta x}{\Delta}\right]^{iy}\right] , \tag{B9}$$

where $\theta = 3s/5 - \pi/4 - y\ln(\Delta/24)$. Matching (B9) to (B10) for $z<0$ in region 2 then yields

$$\Psi_2 = AD_\nu^- - BD_\nu^+ , \tag{B10}$$

where

$$\begin{aligned} A &= \frac{\Gamma(\frac{1}{2}+iy)}{\sqrt{2\pi}}\left[\frac{4}{\Delta}\right]^{iy} (2s)^{1/4-iy/2} \\ &\quad \times e^{-i\theta}\left[\frac{q_0}{s}\right]^{1/2} e^{-3\pi i/8} e^{-3\pi y/4} \\ &\quad \times \left[1 + e^{2i\theta} e^{\pi i/2} e^{\pi y/2} (2s)^{iy}\left[\frac{4}{\Delta}\right]^{-2iy} \frac{\sqrt{2\pi}}{\Gamma(\frac{1}{2}+iy)}\right] , \end{aligned} \tag{B11}$$

$$\begin{aligned} B &= \frac{\Gamma(\frac{1}{2}+iy)}{\sqrt{2\pi}}\left[\frac{4}{\Delta}\right]^{iy} (2s)^{1/4-iy/2} \\ &\quad \times e^{-i\theta}\left[\frac{q_0}{s}\right]^{1/2} e^{-7\pi i/8} e^{\pi y/4} . \end{aligned}$$

Having determined the linear combination of $D_\nu^\pm$ around the barrier top, we analytically continue (B10) into region 1 for z large and positive. Matching the wave function to ($B4'$) then gives us the equal weight superposition of incoming and outgoing wave of the scattering state.

$$\Psi_1 = A_1\Psi_1^- + B_1\Psi_1^+ , \tag{B12}$$

where

$$A_1 = (2s)^{-1/2(1/2+iy)} e^{\pi y/4} e^{-\pi i/8} \times (Ae^{-\pi y} e^{\pi i/2} - B) \left[\frac{4}{\Delta}\right]^{iy} e^{-iy/2} ,$$

$$B_1 = -(2s)^{1/2(iy-1/2)} e^{-\pi y/4} e^{7\pi i/8} \times \frac{\sqrt{2\pi}}{\Gamma(\frac{1}{2}+iy)} Ae^{-iy} e^{-iy/2} = -A_1^* .$$

This completes the calculation of the wave function in all three regions.

[1]A. O. Caldeira and A. J. Leggett, Ann. Phys. (N.Y.) **149**, 374 (1983).

[2]V. Ambegaokar, in *Proceedings of the NATO Advanced Study Institute on Percolation, Localization and Superconductivity, Les Arcs, 1983,* edited by A. M. Goldman and S. A. Wolf (Plenum, New York, 1984).

[3]U. Eckern, G. Schön, and V. Ambegaokar, Phys. Rev. B **30**, 6419 (1984).

[4]M. H. Devoret, J. M. Martinis, and J. Clarke, Phys. Rev. Lett. **55**, 1908 (1985).

[5]J. M. Martinis, M. H. Devoret, and J. Clarke, Phys. Rev. Lett. **55**, 1543 (1985)

[6]M. H. Devoret, J. M. Martinis, Daniel Esteve, and J. Clarke, Phys. Rev. Lett. **53**, 1260 (1984).

[7]D. A. Browne, K. S. Chow, and V. Ambegaokar, Phys. Rev. B **35**, 7105 (1987).

[8]A. I. Larkin and Yu. N. Ovchinnikov, Pis'ma. Zh. Eksp. Teor. Fiz. **91**, 318 (1986) [Sov. Phys.—JETP **64**, 185 (1986)].

[9]A. I. Larkin and Yu. N. Ovchinnilov, J. Low Temp. Phys. **63**, 317 (1986).

[10]M. H. Devoret, J. M. Martinis, Daniel Esteve, and J. Clarke (private communication).

[11]D. Esteve, M. H. Devoret, and J. M. Martinis, Phys. Rev. B **34**, 158 (1986).

[12]A. Schmid, J. Low Temp. Phys. **49**, 609 (1982).

[13]U. Eckern and F. Pelzer, Europhys. Lett. **3**, 131 (1987).

[14]D. C. Langreth, in *NATO Advanced Study Institute Linear and Nonlinear Electron Transport in Solids* (Plenum, New York, 1976), Vol. 17, p. 3.

[15]A. J. Leggett, S. Chakravarty, A. T. Dorsey, M. P. A. Fisher, A. Garg, and W. Zwerger, Rev. Mod. Phys. **59**, 1 (1987).

[16]V. Ambegaokar and U. Eckern, Z. Phys. B **69**, 499 (1987).

[17]W. Bialek, S. Chakravarty, and S. Kivelson, Phys. Rev. B **35**, 120 (1987).

[18]H. A. Kramers, Physica **7**, 284 (1940).

[19]A. J. Leggett, Phys. Rev. B **30**, 1208 (1984).

[20]I. Affleck, Phys. Rev. Lett. **46**, 388 (1981).

[21]A. I. Larkin and Yu. N. Ovchinnikov, Pis'ma Zh. Eksp. Teor. Fiz. **37**, 322 (1983) [Sov. Phys.—JETP **37**, 382 (1983)].

[22]H. Grabert and U. Weiss, Phys. Rev. Lett. **53**, 1787 (1984).